

Final career project

Electronic, Robotic and Mechatronic Engineering

Development of a graphical simulator for microgrids
with renewable energies.

Author: Luis Marzo Román

Supervisors: Carlos Bordons Alba
Luis Valverde Isorna

**Department of Systems and Automatic
Department of Energetic Engineering
Higher Technical School of Engineering
University of Seville**

Seville, 2017



Final career project
Electronic, Robotic and Mechatronic Engineering

Development of a graphical simulator for microgrids with renewable energies.

Author:

Luis Marzo Román

Tutors:

Carlos Bordons Alba

Luis Valverde Isorna

Department of Systems and Automatic
Department of Energetic Engineering
Higher Technical School of Engineering
University of Seville

Sevilla, 2017

To my family

To my teachers

Acknowledgements

I would like to express my gratitude to my family for their support during these four long and endless years of university career and my friends who have accompanied me on this complicated journey.

This work would not have been possible without the great knowledge of Luis Valverde and Carlos Bordons, my tutors whom I appreciate for all the time they have invested in me.

Finally, I would like to thank Laura for the suffering and to endure my innumerable annoyances in the accomplishment of this work.

Thank you all.

Luis Marzo Román

Seville, 2017

Resumen

Actualmente el planeta está pasando por una crisis energética. La mayoría de la energía consumida en el mundo proviene de los combustibles fósiles tales como petróleo o carbón. Estos combustibles para que se transformen en sustancias de gran contenido energético tardan millones de años en producirse, y poco a poco se están agotando.

Las energías renovables y la nueva “economía de hidrógeno” podría ser la solución. Gran cantidad de científicos ya están desarrollando nuevas tecnologías tales como almacenamiento energético basado en hidrógeno para luchar por el cambio.

Para alcanzar dichos objetivos, en este trabajo vamos a empezar estudiando sistemas de generación de energías renovables, más tarde sistemas de almacenamiento de energía eléctrica y concluiremos montando una microrred con un sistema de control complejo.

Este trabajo servirá como base a futuras investigaciones sobre sistemas basados en hidrógeno. Por lo cual, creemos que una interfaz gráfica de la microrred con el usuario podría ayudar con las múltiples posibilidades de sistemas que podemos llegar a montar en nuestras simulaciones.

Abstract

Currently there is an energy crisis on the planet. Most of the energy consumed in the world comes from fossil fuels such as oil or coal. These fuels take millions of years to be transformed into substances of great energetic content, and slowly they are being exhausted.

Renewable energies and the new "hydrogen economy" could be the solution. Many scientists are already developing new technologies such as hydrogen-based energy storage to change this alarming situation.

To achieve these objectives, in this work we will start studying renewable energy generation systems, later electrical energy storage systems and we will conclude by creating a microgrid with a complex control system.

This work will serve as a basis for future research on hydrogen-based systems. Therefore, we believe that a graphical interface of the network with the user could help with the infinite possibilities of systems that we can simulate.

Index

Acknowledgements	ix
Resumen	xi
Abstract	xiii
Index	xiv
Index of tables	xvi
Index of figures	xvii
1 Introduction	11
1.1. <i>Introduction</i>	11
1.2. <i>Goals</i>	12
1.3. <i>Methodology</i>	12
2 Types of systems	15
2.1. <i>Wind turbine</i>	15
2.1.1 Wind turbine model	16
2.2. <i>Photovoltaic cell</i>	19
2.2.1 Mathematical model of a photovoltaic cell	20
2.2.2 Simulink implementation	22
2.3. <i>Gas microturbine</i>	23
2.3.1 Gas microturbine model	24
2.4. <i>PEM electrolyser</i>	28
2.4.1 PEM electrolyser model	29
2.4.2 Hydrogen flow rate	31
2.4.3 Simulink implementation	31
2.5. <i>Metal hydride</i>	33
2.5.1 Metal hydride model	34
2.5.2 Mass and energy balance	35
2.5.3 Process kinetic	37
2.5.4 Simulink implementation	38
2.6. <i>Fuel cell</i>	41
2.6.1 Fuel cell model	43
2.6.2 Electrochemical model	43
2.3.1 Simulink implementation	45
2.7. <i>Stationary battery</i>	46
2.7.1 Stationary battery model	47
2.7.2 Simulink implementation	49
3 Complete system and user interface	51
3.1. <i>Energy demand model</i>	51
3.2. <i>Control system model</i>	52
3.3. <i>Complete model</i>	55
3.4. <i>User interface</i>	55
4 Analysis and conclusions	59

<i>4.1. Analysis</i>	59
<i>4.2. Conclusions</i>	64
Bibliography	65

INDEX OF TABLES

Table 1. Technical characteristics for the wind turbine AIR 403

Table 2. Technical characteristics of the module

Table 3. Mathematical coefficients

Table 4. PEM electrolyser characteristic

Table 5. Metal hydride parameters.

Table 6. X_i coefficient

Table 7. Parameters of the lead-acid battery model

INDEX OF FIGURES

- Figure 1. Horizontal axis wind turbines*
- Figure 2. Power curve.*
- Figure 3. Simulink model AIR 403*
- Figure 4. Simulation power curve.*
- Figure 5. Electric current on photovoltaic cells*
- Figure 6. Circuit model of a photovoltaic cell*
- Figure 7. I-V curves at different temperature.*
- Figure 8. I-V curves at different irradiance*
- Figure 9. Elements of a gas turbine*
- Figure 10. Thermodynamic cycle*
- Figure 11. Power generated by microturbine*
- Figure 12. Water electrolysis.*
- Figure 13. Simulink model of PEM electrolyser.*
- Figure 14. Simulink PEM electrolyser model.*
- Figure 15. I-V curve of PEM electrolyser*
- Figure 16. Hydrogen flow produced by PEM electrolyser.*
- Figure 17. Metal hydride*
- Figure 18. Metal hydride simulink charge.*
- Figure 19. Metal hydride simulink model. Discharge.*
- Figure 20. Pressure in the hydride.*
- Figure 21. Temperature in the charge process*
- Figure 22. Temperature in the discharge process.*
- Figure 23. Fuel cell model*
- Figure 24. Simulink fuel cell model*
- Figure 25. Fuel cell I-V curve*
- Figure 26. Hydrogen flow consumed.*
- Figure 27. Scheme for loading and unloading a lead-acid battery*
- Figure 28. Electrical schematic for the battery model*
- Figure 29. Simulink battery model*
- Figure 30. Output voltage of the battery against current step*
- Figure 31. Electric energy demand in Spain. Source: Red eléctrica Española.*
- Figura 32. Power demand for an average home*
- Figure 33. Control system.*
- Figure 34. Schematic of network operation*
- Figure 35. Flowchart.*
- Figure 36. Complete system.*
- Figure 37. User interface*

Figure 38. User interface parameters.

Figure 39. First system simulation

Figure 40. Second system simulation

Figure 41. Third system simulation

Figure 42. Fourth system simulation

Figure 43. Fifth system simulation

Figure 44. Sixth system simulation

Figure 45. Seventh system simulation.

Figure 46. Real wind profile.

Figure 47. Real cloudy profile.

Figure 48. Real sunny profile.

CHAPTER 1

Introduction

Index

1.1. Introduction.....	11
1.2. Goals.....	12
1.3. Methodology.....	12

1.1. Introduction

Currently investing in renewable energy systems is an indispensable measure for the sustainability of the planet's resources. Renewables are sources of clean, inexhaustible and increasingly competitive energy.

The great interest that is being generated by renewable energies is due to the fact that these sources help to reduce emissions of greenhouse gases, contribute to the creation of employment and technological development.

Hydrogen plays a key role in the sustainability of resources. It is what is called "hydrogen economy", where hydrogen would be used as a source of energy and transformed into electricity. With hydrogen, generated cleanly and economically, we would reduce dependence on fossil fuels and reduce air pollution.

However, implementing this Hydrogen Economy is not easy. Current methods for producing hydrogen are costly and rely on the gasification of fossil fuels at high temperatures and pressures. In addition, storing all this hydrogen is a big problem because large volumes of hydrogen are needed because of the low energy density of hydrogen. It is currently being investigated with metal hydrides and storage tanks at high pressures for efficient fuel storage.

1.2. Goals

The objective is clear: **We are going to develop a graphical simulator for microgrids with renewable energies.**

This work is motivated by the great importance of renewable energy and the sustainability of the planet in the future. In addition, this work opens several research lines due to the systems we are currently dealing with are continuously being updated and therefore new control strategies will emerge.

To begin with, we will study individual systems, identify different modes of operation, and implement different control strategies in our entire system. Finally, we will analyze the results obtained.

In this work we wanted to reproduce the systems under real operating conditions and for this reason we have used real technical data in our simulations.

1.3. Methodology

The methodology is organized in the following points:

1. Study and analysis of hydrogen storage systems and renewable energy production systems.
2. Mathematical modeling of all power and storage systems.
3. Implementation and simulation of these systems in Simulink programming environment.
4. Construction of a microgrid model with all the systems mentioned above.
5. Construction of graphical user interface for the microgrid simulation.
6. Programming of different operating modes of the micro-grid.
7. Evaluation of the complete microgrid performance.

❖ **FIRST STAGE: Study and analysis.**

In this first stage we will look for information of all the systems of production and storage of renewable energy. We will have an idea of how they work, their advantages and disadvantages and how we could use and implement them in our microgrid.

We will look for technical documents where the same subject has been previously approached to have a general idea of the problems that we can find. In addition we will review different control strategies that we can use in our microgrid to obtain an optimal operation.

❖ SECOND STAGE: Mathematical model.

We will develop mathematical models of the energy production and storage systems that will be used in our microgrid. We will validate them by comparing them with available data on the literature.

❖ THIRD STAGE: Implementation.

These mathematical models will be implemented in a computer programming software called Matlab-Simulink. With this, we will obtain the characteristic curves of each system and we will see how they react to different events.

❖ FOURTH STAGE: Construction of the microgrid.

The most complicated part of the work is the construction of the complete system. We must merge all the individual systems and see the operation of the microgrid. We will develop a new system that will be in charge of controlling the entire network. We will implement different control strategies and analyze the results.

❖ FIFTH STAGE: User interface.

We will program a flexible graphical user interface so that the user does not have to touch anything in simulink so the user can make simulations of the microgrid in an easy and simple way.

❖ SIXTH STAGE: Evaluation and conclusions.

We will make several simulations to see how the microgrid reacts to different events. We will extract conclusions from the data obtained and we will talk about future work.

CHAPTER 2

Types of systems

Index

2.1. Wind turbine	15
2.2. Photovoltaic cell	19
2.3. Gas microturbine	23
2.4. PEM electrolyser	28
2.5. Metal hydride	33
2.6. Fuel cell	41
2.7. Stationary battery	46

5.1. Wind turbine

A wind turbine is defined like an electrical energy generator that works thanks to wind power. The most common and efficient are the horizontal axis wind turbines, but also exist vertical axis wind turbine.

A wind turbine usually needs a minimal speed of 3 or 4 m/s for start working. The operation of the turbine is very simple. First of all, we have to guide correctly the blades to improve the wind power. The blades will start spinning with a speed between 4 m/s and 11 m/s, and if the wind speed is higher than 25 m/s, we must change the orientation of the blades to avoid a possible break of the turbine.



Figure 1. Horizontal axis wind turbines

The components of the wind turbine are:

- Tower: The tower raises the generator and the blades to a high altitude to generate a huge amount of energy.
- Rotor and the blades: The blades are usually made of polyester with fiberglass reinforcement for high strength. The length is between 40 and 80 meters. When the wind spins the blades, they transform the kinetic energy into a torque along the rotor axis.
- Nacelle: Is the space where all the mechanical and electrical elements are.
- Gearbox: His main function is to modify the speed of the main axis to be suitable for the generator.
- Generator: This system convert the energy into electricity. There are different types of generators like the synchronous generator or induction biphasic generator.
- Brake system: We use the brake system to block the turbine when the wind speed is too high.
- Control system: This system manage the information about the state of the wind turbine or the correctly operation of the turbine.

5.1.1. Wind turbine model

The wind potential is the capacity of the wind turbine to obtain energy. This is determined by variables such as power density (how much energy we get at different wind speeds), whether the wind turbine is fixed or variable pitch or by the Weibull distribution, which indicates the probability over a year and in a specific area that the wind blows at a certain speed.

Theoretically the maximum energy that a turbine can get from the wind independently of the design is 60%. This is the Betz limit. We can see in the figure 2 the Betz limit and the generated power by a fixed pitch wind turbine (green area) and a variable pitch wind turbine (red curve).

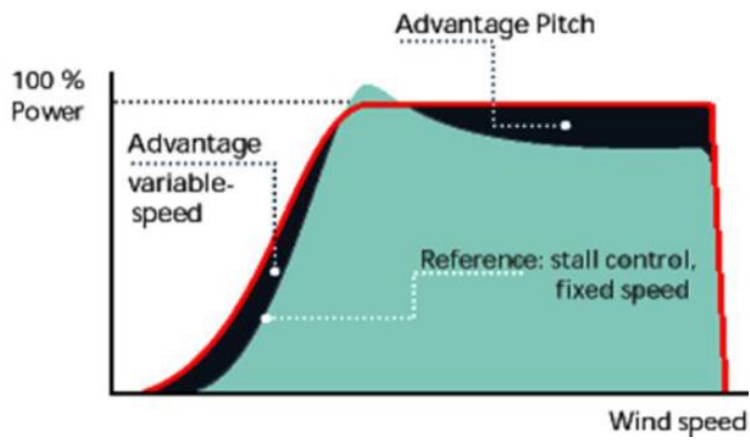


Figure 2. Power curve.

In the simulation, we will use the wind turbine Air 403.

Table 1. Technical characteristics for the wind turbine AIR 403

Wind turbine Air 403	
Nominal Power (W)	400
Number of blades	3
Weight (Kg)	5.85
Nominal wind speed (m/s)	12.5
Minimal wind speed (m/s)	2.7
Length of the blades (m)	0.585

The wind power is determinate by the following equation:

$$P = \frac{1}{2} \rho A v^3 C_p(\varepsilon, \theta)$$

Where

P is the power of the win (W).

A is the area of the rotor (m^2)

V is the wind speed (m/s)

ρ is the air density (kg / m^3)

$Cp(\varepsilon, \theta)$ is a coefficient as a function of the blade speed ε and the blade angle.

The dynamics of the wind turbine is due to the inertia of the rotor. We will use a second order system to model the behaviour of the turbine (Luis Valverde, 2013). The transfer function is:

$$\frac{Pg}{Pwt} = \frac{0.25}{s^2 + 0.707s + 0.25}$$

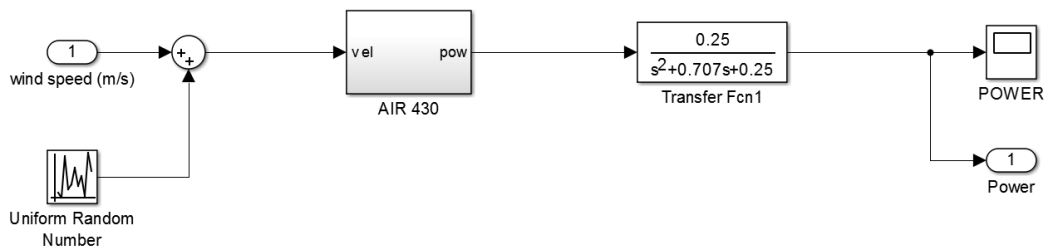


Figure 3. Simulink model AIR 403

At the entrance of our system we will add random numbers to simulate the randomness of the wind gusts. We will represent the step response to observe the dynamics of the system. The wind speed at the entrance will be 10 m / s and after 60 seconds we will change the reference to 15 m / s.

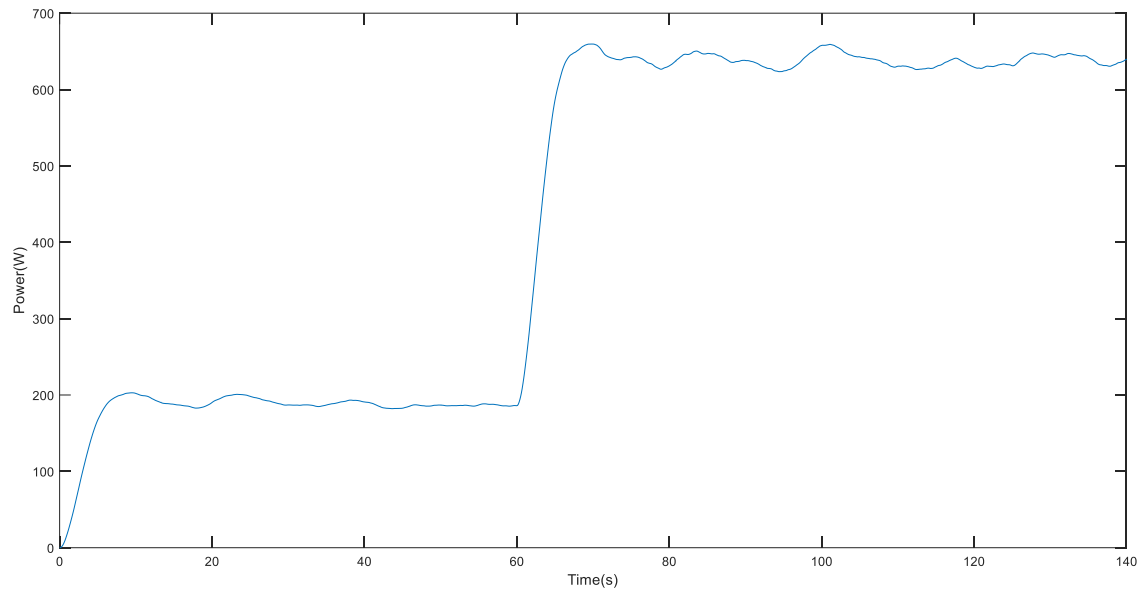


Figure 4. Simulation power curve.

5.2. Photovoltaic cell

Photovoltaic cells are electronic devices that convert solar energy into electrical energy. Light falls on a semiconductor device normally made of silicon and composed of two layers producing a voltage difference between them. When the voltage is able to conduct a current through the circuit, useful work is produced.

Photovoltaic cells are formed by p-type and n-type silicon. When a photon reaches the cell, it ionizes the atoms in the silicon and separates an electron (negative charge) that creates at the same time a gap (positive charge). The gaps move towards the positive layer or the p-layer and the electrons move towards the negative or the n-layer, thus a potential difference occurred.

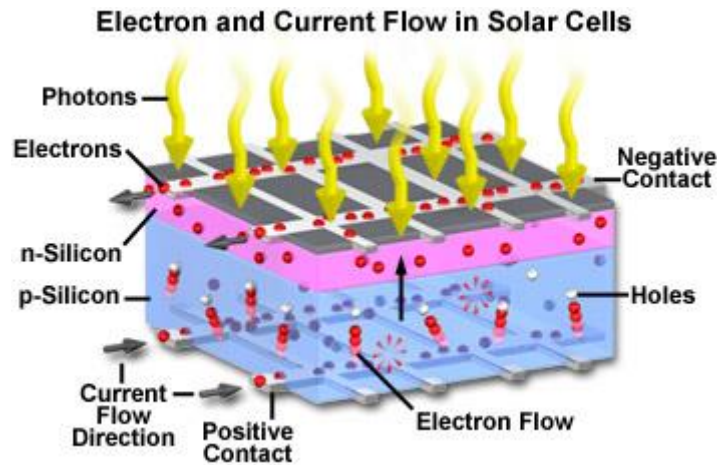


Figure 5. Electric current on photovoltaic cells

Electrical data provided by manufacturers about their cells under standard measurement conditions are $1000\text{W} / \text{m}^2$ and $T = 25^\circ \text{C}$. Some of these technical specifications are:

The short-circuit current (I_{cc}): it is the current obtained between the terminals of a solar panel when there is no resistance. In other words, it is the maximum intensity that can be recorded between both terminals.

The open circuit voltage (V_{ca}): it is the maximum voltage value at the ends of the cell and occurs when it is not connected to any load.

Peak power (W_p): It is the product of the value of voltage and maximum intensity for which the power delivered to the load is maximum.

5.2.1. Mathematical model of a photovoltaic cell

The behavior of a cell when it functions as a current generator can be explained as the difference in the photogenerated current and the diode current (Alejandro J. Del Real, 2007). The electric current generated is:

$$I = I_L - I_D$$

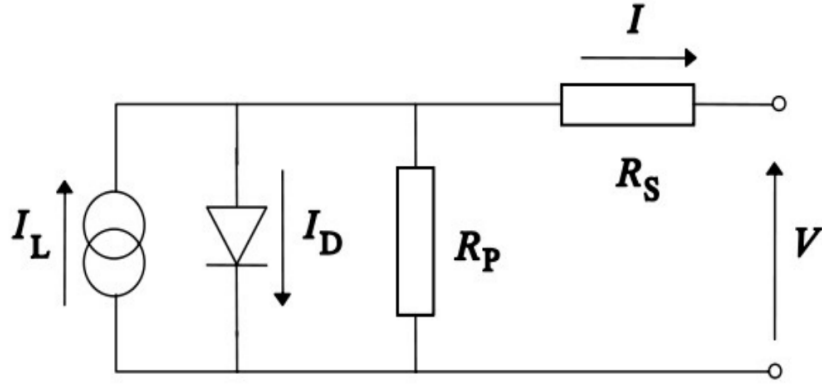


Figure 6. Circuit model of a photovoltaic cell

Developing the first equation, we obtain the following expression:

$$I = I_L - I_o \exp\left(\frac{V + IR_s}{mV_t} - 1\right) - \left(\frac{V + IR_s}{R_p}\right)$$

$$V_t = \frac{kT_c}{e}$$

Where

I_L is the photogenerated electric current (A)

I_o is the saturation current of the diode (A)

R_s is the series resistance (Ω)

R_p is the parallel resistance (Ω)

m is the ideal factor of the diode

V_t is the thermal voltage

k is the Boltzman's constant

T_c is the temperature of the cell (K)

e is the electron charge

To simulate our system we will assume some simplifications. The new photovoltaic cells have the characteristic that the form factor is high, so the parallel resistance is very high in relation to the series resistance. In addition, the current I_L can be approximated by the short circuit current. With these simplifications we can write the previous equation as:

$$I_{sf} = I_{sc_{sf}} \left(1 - e^{\left(\frac{V_n - V_{oc_{sf}} + I_{sf} R_s}{V_T} \right)} \right) - \frac{V_n + I_{sf} R_s}{R_p}$$

$$V_{oc} = m \frac{KT}{e} \ln \left[\frac{I_L}{I_o} + 1 \right]$$

$$I_{sc_{sf}} = \frac{I_{sc} n p_{sf} G}{1000}$$

Where

V_n is the nominal voltage of the photovoltaic generator (V)

$I_{sc_{sf}}$ is the generator short circuit current (A)

$V_{oc_{sf}}$ is the generator open circuit voltage (V)

V_T is the voltage dependent of the temperature (V)

R_s is the series resistance (Ω)

R_p is the parallel resistance (Ω)

G is the incident irradiance on the cell (W/m²)

5.2.2. Simulink implementation

For the simulation we have chosen the technical data of the photovoltaic generator Isofoton® I-106/12

Table 2. Technical characteristics of the module

Isofoton® module I-106/12	
Peak power on the module (W)	106
Intensity in the maximum power point (A)	6.10
Short circuit current (A)	6.54
Voltage in the maximum power point (V)	17.4

To verify the model, we represent the I-V curve at different temperatures and at different irradiances.

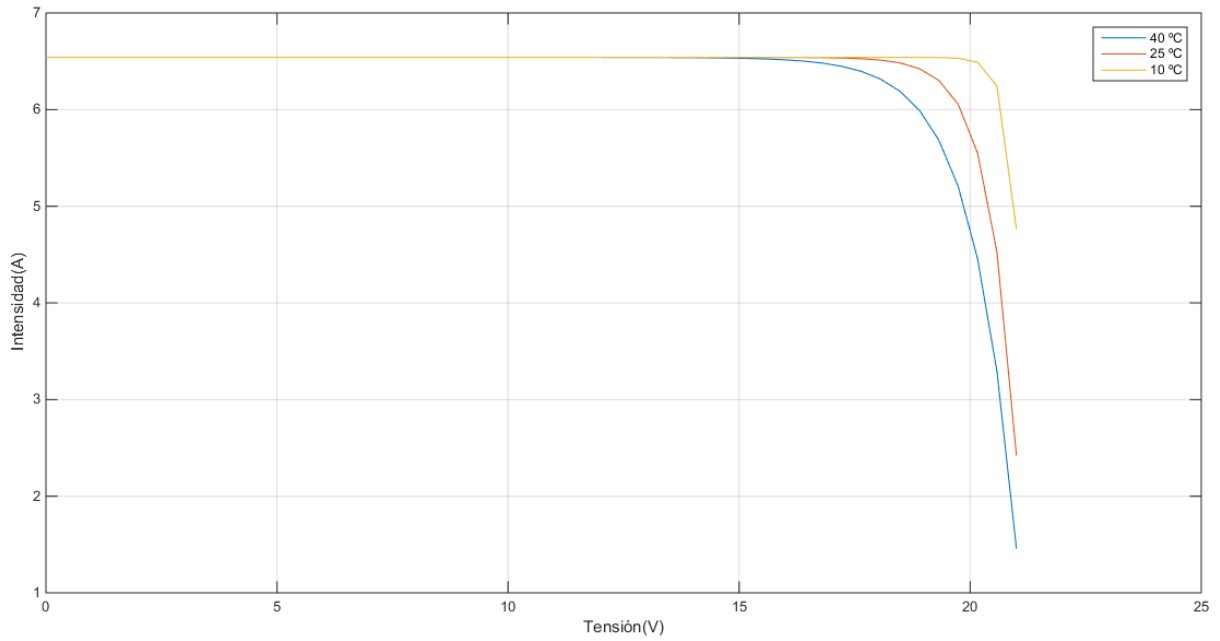


Figure 7. I-V curves at different temperature.

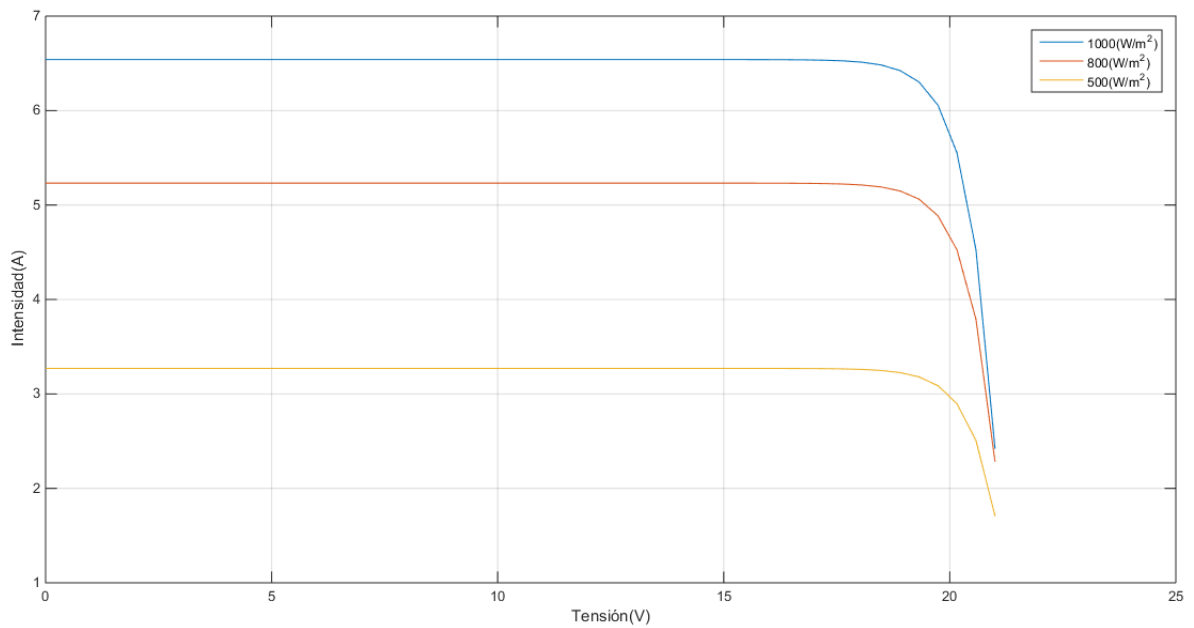


Figure 8. I-V curves at different irradiance.

5.3. Gas microturbine

The gas turbine, also called combustion turbine, is a type of internal combustion engine which consists of a turbocharger, a combustion chamber and a gas turbine.

The compressor obtains atmospheric air (state 1) and compresses it to a pressure p_2 . This compressed air enters in the combustion chamber operating at constant pressure to generate gases at high temperatures (state 3). For this, a liquid or gaseous fuel is injected. These gases expand in the gas turbine up to atmospheric pressure (state 4), generating a motor work that we can convert into electrical power.

When the evolution of the working fluid in the compressor and the turbine is close enough to the ideal conditions and the temperature of the gases in the turbine are high, the turbine engine work is greater than the work of the compressor. Therefore, surplus labor constitutes the useful work of the machine

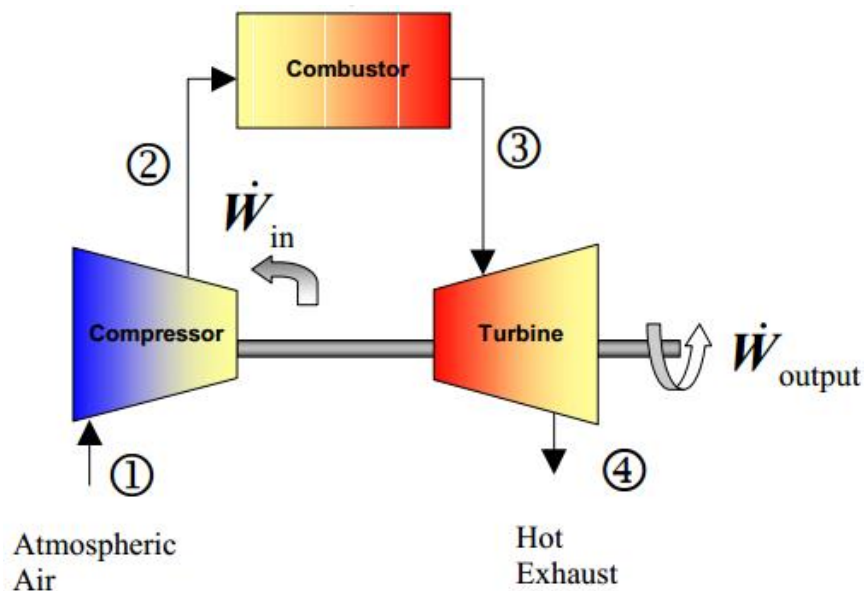


Figure 9. Elements of a gas turbine

Gas microturbines are combustion engines that are based on the same principle as conventional turbines but simplifying mechanical elements. As regards the thermodynamic part, the microturbine follows a Brayton Regenerative cycle: it improves its electrical performance by using a heat exchanger of the gases at the exit of the combustion chamber to preheat the combustion air after the compressor.

5.3.1. Gas microturbine model

We will study the mathematical models that describe the processes of the gas turbine. The thermodynamic cycle performed by the fluid is as follows (Toledo Velazques, 2010):

Isentropic process: ambient air is drawn into the compressor, where it is pressurized (1-2s).

1. Isobaric process: the compressed air then runs through a combustion chamber, where fuel is burned (2s-3).
2. Isentropic process: the heated, pressurized air then gives up its energy, expanding through a turbine (3-4s).
3. Isobaric process: heat rejection (4s-1)

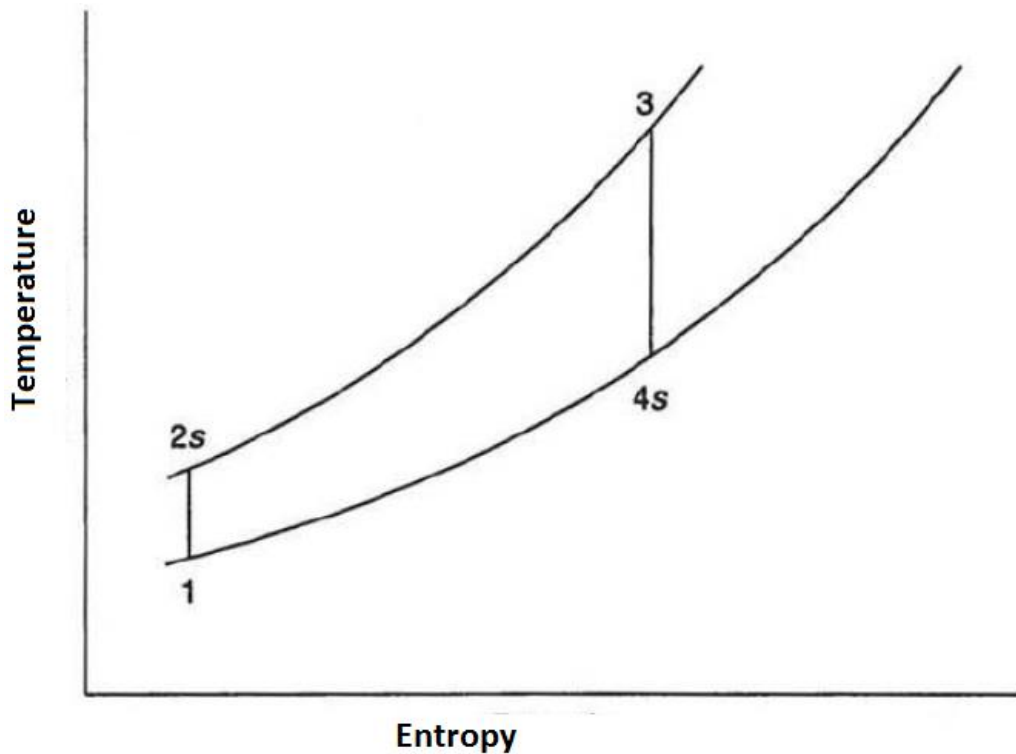


Figure 10. Thermodynamic cycle

The generated power that produces the complete cycle is given by:

$$P_{TG} = W_M \cdot \dot{m}_a$$

$$W_M = W_{TG} - W_C$$

Where

W_M is the motor work (W)

W_{TG} is the work done by the turbine (W)

W_C is the work done by the compressor(W)

\dot{m}_a is the air flow (kg/s)

The work that is supplied to the compressor and the turbine can be calculated from the following expressions:

$$W_C = C_p T_1 (z^x - 1)$$

$$W_{TG} = C_p T_3 \left(1 - \frac{1}{z^x} \right)$$

Where

C_p is the specific heat of the air J/(kg K)

T_1 is the atmospheric temperature (K)

T_3 is the temperature at the exit of the combustion chamber (K)

z is the ratio of pressures in the compression chamber

x is the ratio between the particular constant and the specific heat of the working fluid

The compression ratio and the temperature in the compression chamber are known from the beginning. However, the temperature at the exit of the combustion chamber depends on the amount of fuel we inject. In our case we will use as methane fuel.

$$\dot{m}_c = \frac{\dot{m}_a (T_3 - T_2)}{PCI}$$

$$T_2 = T_1 \cdot \left(\frac{p_2}{p_1} \right)^{\left(\frac{k-1}{k} \right)}$$

Where

\dot{m}_c is the fuel flow injected (Kg/s)

PCI is the calorific value of methane (KJ/Kg)

T_2 is the temperature at the exit of the compression chamber (K)

k is the adiabatic index of air.

To calculate the other variables, we will use the air properties such as the molecular weight, the particular air constant and the adiabatic index of the air.

$$X = \frac{k-1}{k}$$

$$R_a = \frac{R_u}{M_a}$$

$$C_p = \frac{kR_a}{k-1}$$

$$z = \frac{p_2}{p_1}$$

Where

R_a is the particular constant of air (J/kg k)

M_a is the molecular weight of air (g/mol)

R_u is the ideal gas constant (J/kg mol)

For the simulation, we used a Siemens SGT-100® turbine.

Table 3. Mathematical coefficients

Parameter	Value
\dot{m}_a	20.6 Kg/s
z	15.6
k	1.4
M_a	29 g/mol
T_1	288 K
PCI	50050 Kj/kg
Efficiency	31%

By simulating a micro turbine with data from a normal turbine, we are going to subject the system to a small fuel step, going from 10 g / s to 30 g / s.

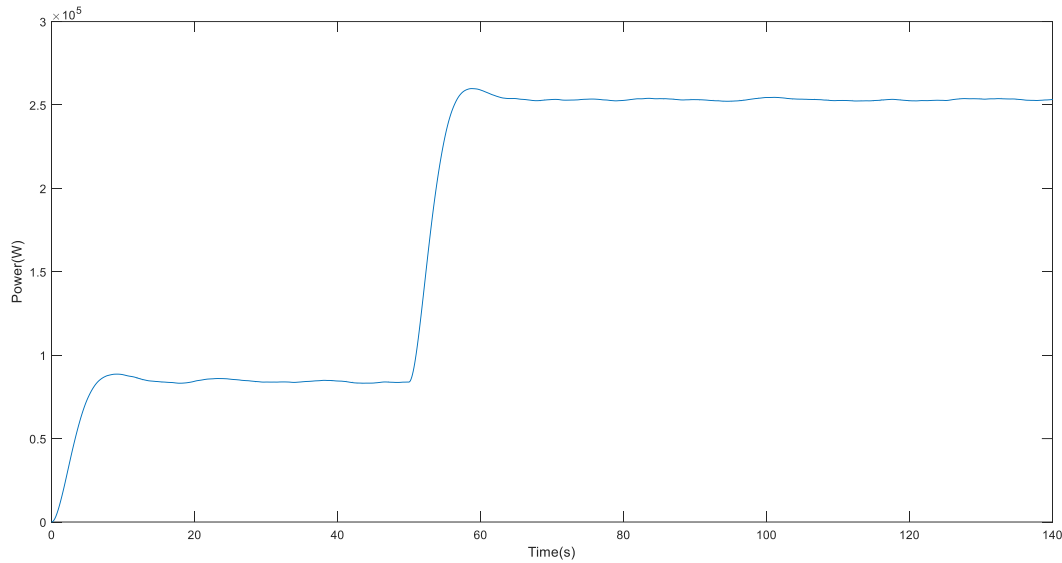
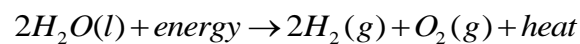


Figure 11. Power generated by microturbine

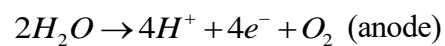
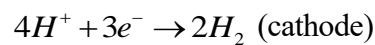
5.4. PEM electrolyser

Electrolysis is an electrochemical process in which water molecule is splitted into hydrogen and oxygen. When an electric current passes through the electrodes, gases are emitted, specifically hydrogen by the cathode and oxygen by the anode. This process takes place in two partial reactions at the electrodes of the system, separated by an electrolyte that is able to conducting ions.

The general expression of the reaction is:



And the semi-reactions involved in the process are:



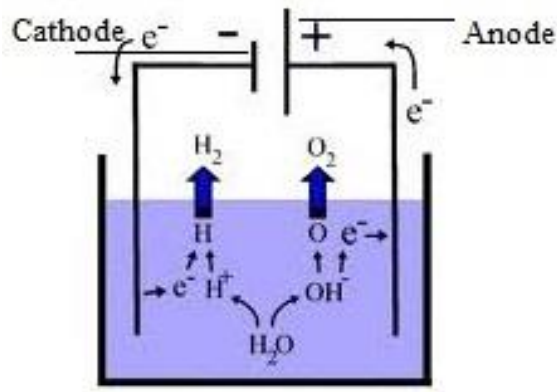


Figure 12. Water electrolysis.

For the maximum efficiency of the electrolytic process, there are two important factors: the total cost of the equipment and the reduction of the energy losses. To do this we will reduce as much as possible the total voltage of the cell to minimize the consumption of electrical energy or we will increase the current density above the normal values to lower the cost of the investment.

Even so, these two objectives are opposed, so it is necessary to optimize the system to adapt it to the operational conditions, because increasing the current density leads to an increase in the total voltage of the cell. In order to produce the electrolysis it is necessary that the potential (V) will be higher than the thermodynamic potential (V_t).

5.4.1. PEM electrolyser model

We will obtain the voltage-current characteristic curve of a cell from the electrochemical model (Luis Valverde, 2013). The total voltage drop in the electrolyser stack is the product of the cells in series and the voltage of the cell. In addition, the voltage drop that is established in the cell is the product of several phenomena, which can be differentiated by the following sums:

$$V_{cell} = V_0 + \eta_{act} + \eta_{ohm} + \eta_{ion}$$

$$V_{stack} = nV_{celda}$$

Where

V_0 is the reversible voltage (V)

η_{act} is the activation potential (V)

η_{ohm} is the voltage drop due to the internal resistance (V)

η_{ion} are the losses related to the ionic concentration (V)

n is the number of cells

The first term is the reversible voltage (V_0). The voltage depends on the temperature and the partial pressures.

$$V_0 = V_{0rev} + \frac{2.3RT \log(P_{H_2}^2 P_{O_2})}{4F}$$

$$V_{0rev} = 1.23 - 0.9^{-3} (T_{stack} - 298)$$

Where R is the ideal gas constant, P_{O_2} and P_{H_2} are the gas partial pressures (bar), T is the temperature in Kelvin and F is the Faraday constant.

The second term is the “Activation potential of the electrodes (η_{act})”:

$$V_{act} = + \frac{RT}{F} \sinh^{-1} \left[\frac{1}{2} (i / i_{ao}) \right] + \frac{RT}{F} \sinh^{-1} \left[\frac{1}{2} (i / i_{co}) \right] + \left(\frac{\delta_B}{\sigma_B} \right) i$$

Where

i is the current density in the stack ($A \text{ cm}^{-2}$)

i_{ao} is the current density at the cathode ($A \text{ cm}^{-2}$)

i_{co} is the current density at the anode ($A \text{ cm}^{-2}$)

δ_B is the width of the electrolyzer membrane (μm)

σ_B is the conductivity of the electrolyser membrane (S/cm). We can calculate it with the following expression:

$$\sigma_B = (0.005139\lambda - 0.00326)e^{1268 \left(\frac{1}{T_{ref}} - \frac{1}{T_{ez}} \right)}$$

The last two terms can be grouped into one, as shown in the following equation:

$$\eta_{ion} + \eta_{ohm} = \eta_{ion_ohm} = \frac{I \delta_B}{A_{stack} \sigma_B}$$

Where A_{stack} is the area of the electrolyser membrane (cm^2).

5.4.2. Hydrogen flow rate

The hydrogen flow rate produced by the electrolyser depends on the current passing through an electrolytic cell and is determined by the following equation:

$$\dot{m}_{H_2} = I_{ez} \frac{n_{ez}}{F}$$

Where

\dot{m}_{H_2} is the flow rate of hydrogen produced $\left(\frac{gr}{h}\right)$

n_{ez} is the number of cells in the stack

I_{ez} is the current in the stack (A)

F is the Faraday constant

5.4.3. Simulink implementation

The electrolyser used for the simulation is the SPE Hydrogen Generator Assembly by United Technologies Hamilton Standard because it is available in the university. The system is an electrolyser of moderate pressure (7 bar), based on SPE water electrolysis technology.

Table 4. PEM electrolyser characteristic

Parameter	Description	Value
A	Stack area	212.35 cm^2
PH_2	Hydrogen partial pressure	6.9 barg
PO_2	Oxygen partial pressure	1.3 barg
I_{o_an}	Anode current density	$1.0631 \cdot 10^{-6}$ A/ cm^2
I_{o_cat}	Cathode current density	$1 \cdot 10^{-3}$ A/ cm^2
δ_m	Membrane thickness	178
σ_m	Membrane conductivity	0.14 S/cm
λ	Humidification	21
C_{ez}	Electrolyser thermal capacity	420400 J/K

The input to the model is the power applied to the stack, and the output is the production of hydrogen. The model is as follows:

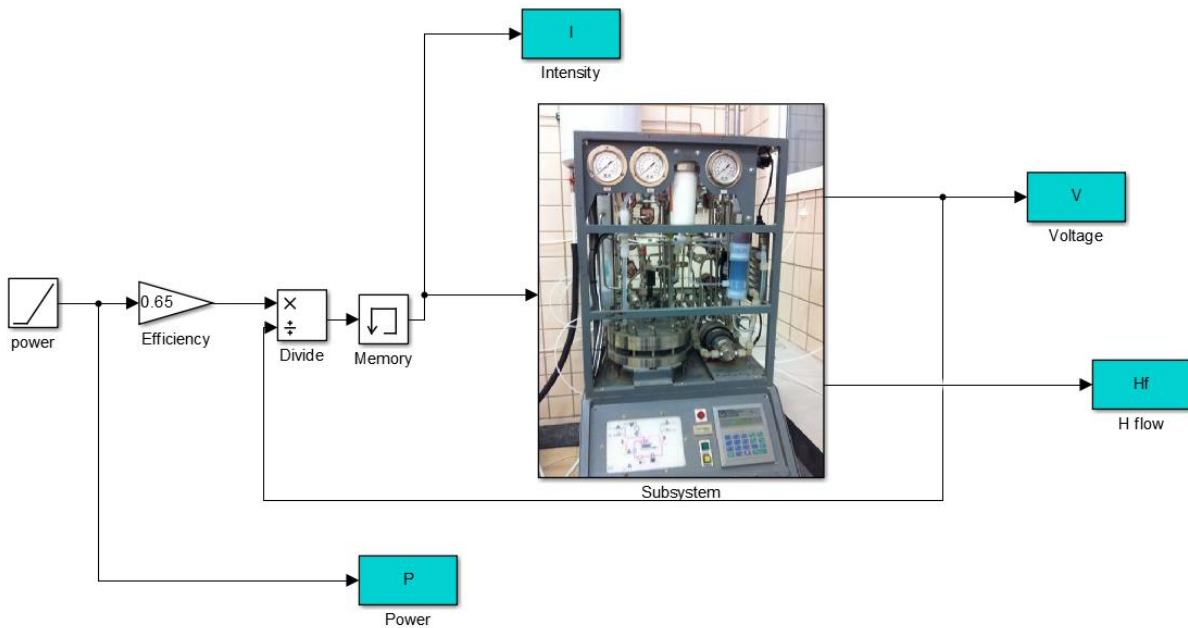


Figure 13. Simulink model of PEM electrolyser.

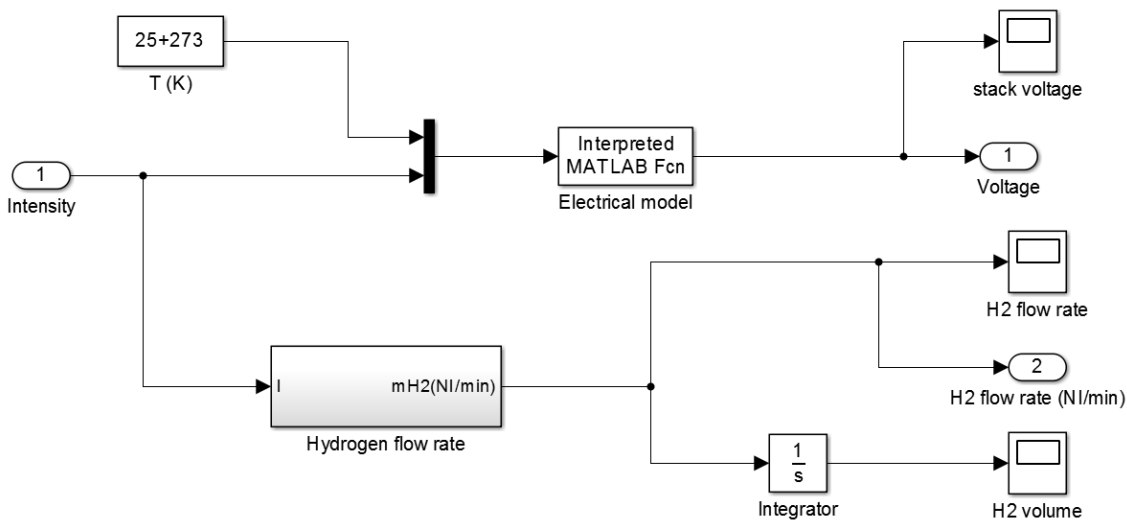


Figure 14. Simulink PEM electrolyser model.

We will apply a power ramp to the electrolyser to see its behaviour. The I-V characteristic of the electrolyser is as follows:

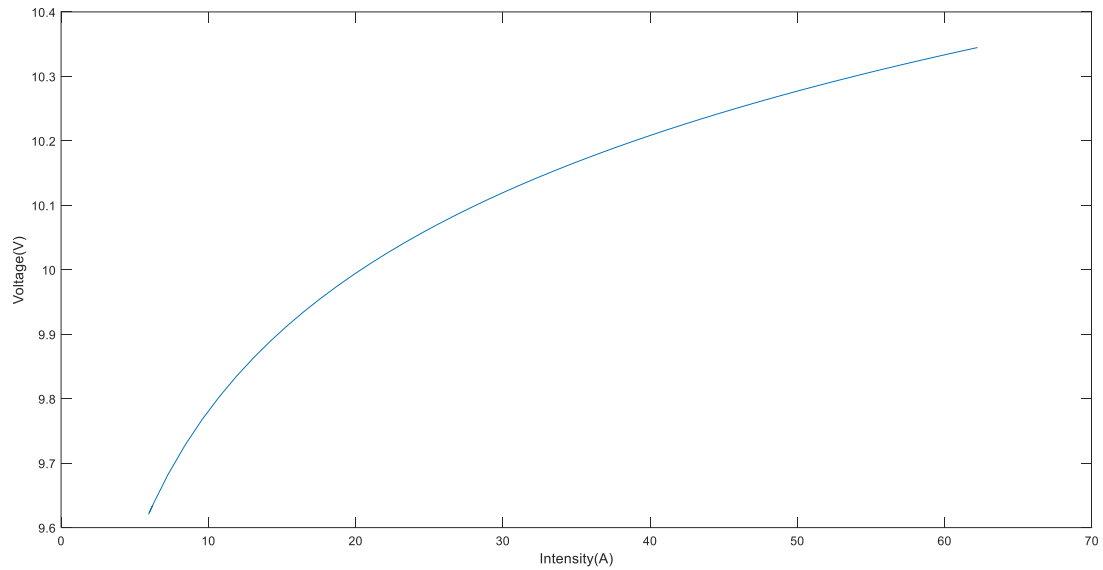


Figure 15. I-V curve of PEM electrolyser

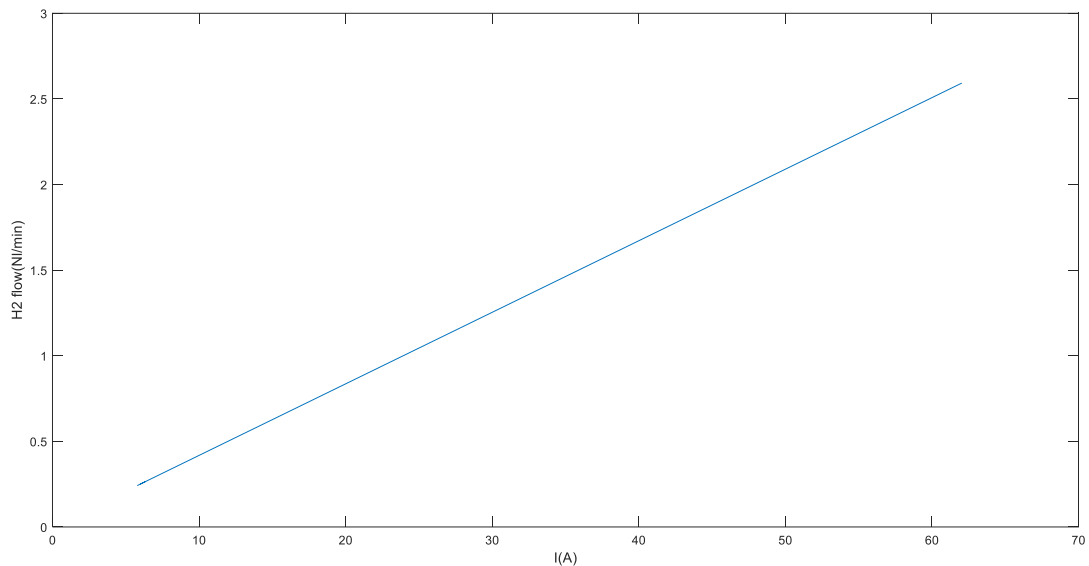
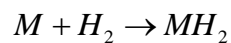


Figure 16. Hydrogen flow produced by PEM electrolyser.

5.5. Metal hydride

The hydrogen economy is an alternative energy model to the use of fossil fuels, in which energy is stored as hydrogen. Certain metals, particularly titanium, iron, manganese, nickel, chromium, etc... may react with the hydrogen to give a metal hydride through an easily controllable reversible reaction. The general equation is as follows:



As the reaction is moderately exothermic, small amounts of heat must be supplied to release the

hydrogen. Even so, different types of metal alloys can be chosen for the hydride, so that the reaction can take place within a wide range of temperatures and pressures.

The reaction takes place to the right, and the metal hydride is formed. This is slightly exothermic and air cooling is usually sufficient. When all the metal has reacted with hydrogen, the pressure will increase. Hydrogen is only stored at moderate pressures, typically around 2 bar.

When the reaction proceeds to the left, the hydrogen is released. If the pressure increases above atmospheric the reaction will be slowly. Now the reaction is endothermic, so you have to supply energy.

Once the reaction is complete and all the hydrogen has been released, the process can be repeated. Normally, several hundred cycles of charge and discharge can be completed. Although hydrogen is not stored under pressure, the container must be able to hand reasonably high pressures (A. Freni, 2009).

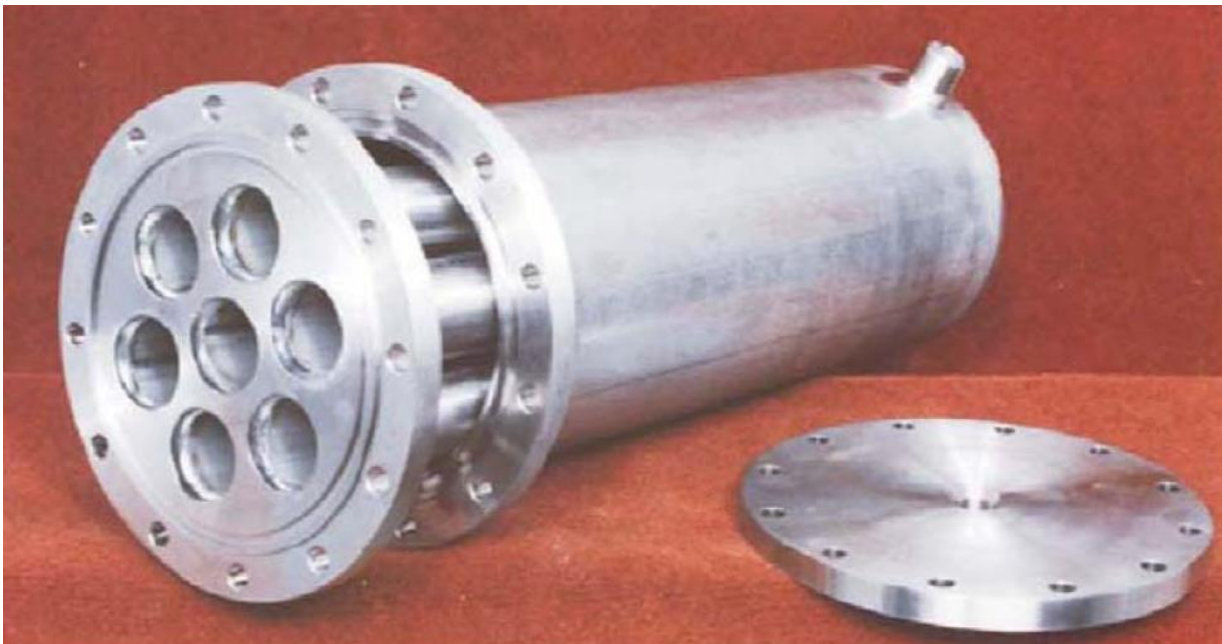


Figure 17. Metal hydride

5.5.1. Metal hydride model

The mathematical model of the metal hydride is very complex. We will assume a series of simplifications and hypotheses (Luis Valverde, 2013):

- Gases are ideal

- Thermophysical properties remain constant
- We neglect the transfer of heat by radiation
- At the beginning of the process, the temperature of the hydride is the same as the temperature of hydrogen.

5.5.2. Mass and energy balance

The following differential equation shows the mass conservation in the charge process:

$$\begin{aligned} \text{❖ Charge:} \quad \dot{m}_{H_{in}} &= \varepsilon_{MH} f V_{bed} \frac{d\rho}{dt} + (1 - \varepsilon_{MH}) \rho_s f V_{bed} \frac{dq_{H2,a}}{dt} \\ \text{❖ Discharge:} \quad \varepsilon_{MH} f V_{bed} \frac{d\rho}{dt} &= -(1 - \varepsilon_{MH}) f \rho_s V_{bed} \frac{dq_{H2,d}}{dt} - \dot{m}_{H2,out} \end{aligned}$$

Where

$\dot{m}_{H2,in}$ is the mass flow rate of hydrogen supplied (Kg s^{-1})

$\dot{m}_{H2,out}$ it is the mass flow rate of hydrogen extracted (Kg s^{-1})

ε_{MH} is the porosity

f is the number of fins

V_{bed} is the volume of the hydride (m^3)

ρ is the hydrogen density (Kg m^{-3})

ρ_s is the metal hydride density (Kg m^{-3})

The flow rate of hydrogen entering the hydride is given by the hydrogen produced from the electrolyser. In contrast, the hydrogen desorbed in the process of discharge is demanded by the fuel cell which produces electric power.

In the equation of charge, the first term represent the accumulated hydrogen ratio in the gas phase, while the second represents the accumulated hydrogen ratio in solid phase.

The hydrogen density follows the next equation:

$$\rho = \frac{P \cdot PM}{RT}$$

Where

R is the ideal gas constant

T is the temperature (K)

P is the pressure (bar)

PM is the molecular weight of hydrogen (2)

The energy balance is described as:

❖ Charge:

$$\left(\rho C_{v,g} + \frac{(1-\varepsilon_{MH})}{\varepsilon_{MH}} q_{H2,a} \rho_s C_{v,g} + \frac{(1-\varepsilon_{MH})}{\varepsilon_{MH}} \rho_s C_{p,s} \right) \frac{dT_{MH}}{dt} = - \frac{(1-\varepsilon_{MH})}{\varepsilon_{MH}} \rho_s \Delta H_a \frac{dq_{H2,a}}{dt} - U_a \frac{A_{cs}}{\varepsilon_{MH} f V_{bed}} (T_{MH} - T_c) + \left(\frac{P_{MH}}{\rho} \right) \frac{m_{H2,in}}{\varepsilon_{MH} f V_{bed}}$$

❖ Discharge:

$$\left(\rho C_{v,g} + \frac{(1-\varepsilon_{MH})}{\varepsilon_{MH}} q_{H2,a} \rho_s C_{v,g} + \frac{(1-\varepsilon_{MH})}{\varepsilon_{MH}} \rho_s C_{p,s} \right) \frac{dT_{MH}}{dt} = - \frac{(1-\varepsilon_{MH})}{\varepsilon_{MH}} \rho_s \Delta H_d \frac{dq_{H2,d}}{dt} + U_d \frac{A_{cs}}{\varepsilon_{MH} f V_{bed}} (T_h - T_{MH}) - \left(\frac{P_{MH}}{\rho} \right) \frac{m_{H2,out}}{\varepsilon_{MH} f V_{bed}}$$

Where

$C_{v,g}$ is the hydrogen specific heat at constant volume ($J K g^{-1} k^{-1}$)

$C_{p,s}$ is the hydride specific heat at constant volume ($J K g^{-1} k^{-1}$)

U_a is the heat transfer coefficient ($W m^2 k^{-1}$)

A_{cs} is the area of heat transfer (m^2)

T_{MH} is the metal hydride temperature (K)

T_C is the cooling temperature (K)

$m_{H_2,in}$ is the mass flow rate of hydrogen supplied ($Kg s^{-1}$)

$m_{H_2,out}$ it is the mass flow rate of hydrogen extracted ($Kg s^{-1}$)

ΔH_a is the enthalpy ($Kj mol^{-1}$)

In the equation of charge, the term to the left of the equal represents the ratio of heat accumulated. The first term on the right side represents the heat ratio involved in the hydrogen absorption process. The second is the heat transfer between the cooling fluid and the hydride, and finally the third represents the heat released when the hydrogen is compressed.

In the discharge, the term on the left of the equal represents the ratio of heat accumulated in the bed. The first term on the right side represents the heat required for the desorption and the last term represents the heat involved in the gas expansion process.

5.5.3. Process kinetic

With the kinetics, we model the rate at which reactions occur in the hydride.

$$\text{❖ Absorption: } \frac{dq}{dt} = C_a e^{\left(\frac{-E_a}{RT}\right)} \ln\left(\frac{P}{P^*}\right) (q_{\max} - q)$$

$$\text{❖ Desorption: } \frac{dq}{dt} = C_a e^{\left(\frac{-E_a}{RT}\right)} \ln\left(\frac{P - P^*}{P^*}\right) (q_{\max} - q)$$

Where

C_a is the pre-exponential constant

E_a is the activation energy ($J molH_2^{-1}$)

R is the ideal gas constant

T is the temperature (K)

P is the gas pressure in the hydride (bar)

P^* is the equilibrium pressure (bar)

q_{\max} is the % p/p of maximum hydrogen that the hydride can contain

To calculate the equilibrium pressure, we use the Van't Hoff equation:

$$\ln P^* = \frac{\Delta H}{RT} - \frac{\Delta S}{R}$$

Where

ΔH is the enthalpy variation(Kj mol^{-1})

ΔS is the entropy variation ($\text{Kj mol}^{-1}\text{K}^{-1}$)

R is the ideal gas constant

T is the temperature (K)

5.5.4. Simulink implementation

The input to the charge model will be the hydrogen pressure. For the discharge model, the input to the model is the hydrogen flow rate demanded by the fuel cell.

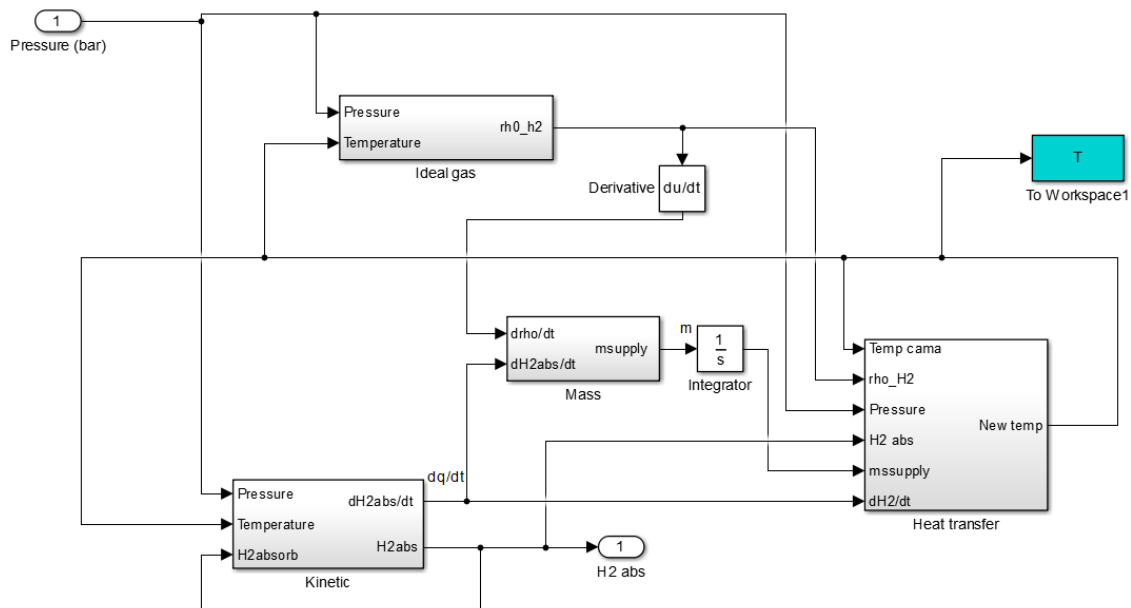


Figure 18. Metal hydride simulink charge.

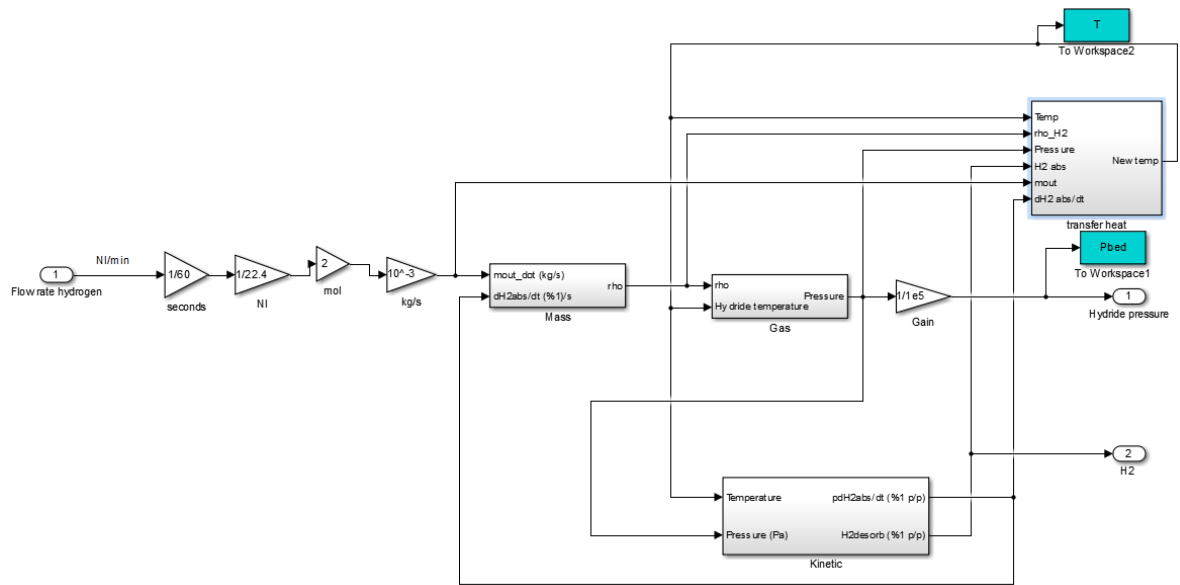


Figure 19. Metal hydride simulink model. Discharge.

For the simulation, we have the technical data of a hydride from LabTech, in particular the model HBond-7000H. This operates at low pressure and temperature, capacity 7000NI and hydrogen delivery rate is in the range of 4.4 - 7 Nm³ / h.

Table 5. Metal hydride parameters.

Parameter	Description	Value
ε	Porosity.	0.5
f	Number of fins.	1 (without fins)
V_{bed}	Metal hydride volume.	0.0380 m ³
ρS	Hydrogen saturated hydride density.	3240 Kg/m ³
ρ	Vacuum hydride density.	3200 Kg/m ³
ΔH	Enthalpy.	30.8 Kj/mol
ΔS	Entropy.	111.5 Kj/mol k
Ea	Activation energy.	21.1796 Kj/mol
C_a	Pre exponential factor.	59.187 (1/seconds)
q_{max}	% Hydrogen weight.	1.2174% p/p
C_{vg}	Specific heat of hydrogen.	14.304 KJ/molK
C_{ps}	Specific heat of metal hydride.	0.419 Kj/molK
A_{cs}	Total heat transfer area.	1.1453 m ²
U	Heat transfer coefficient.	2737 W/m ² K

For the simulation of the charging process we will apply a constant value pressure to the hydride. We will apply a constant input of 4.5 bar. For the discharge process, instead of pressure the input will be a constant hydrogen demand.

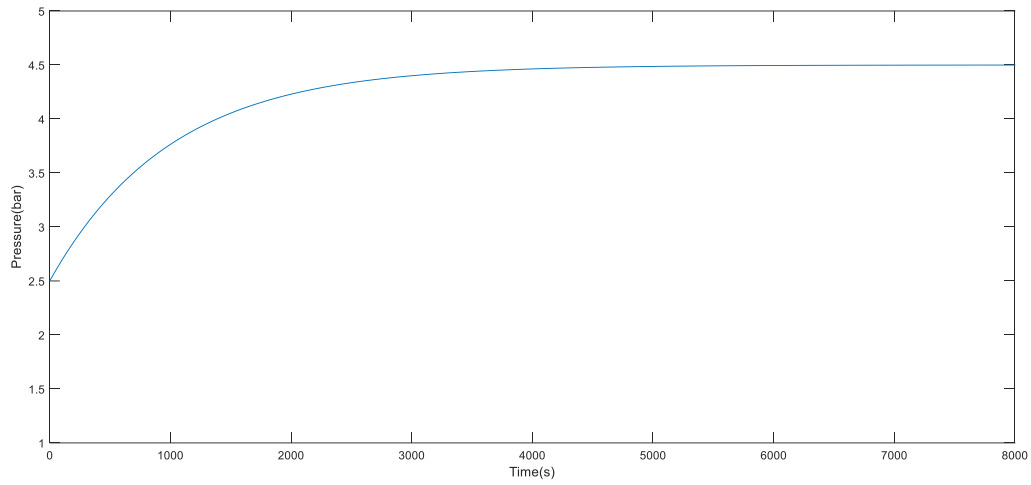


Figure 20. Pressure in the hydride.

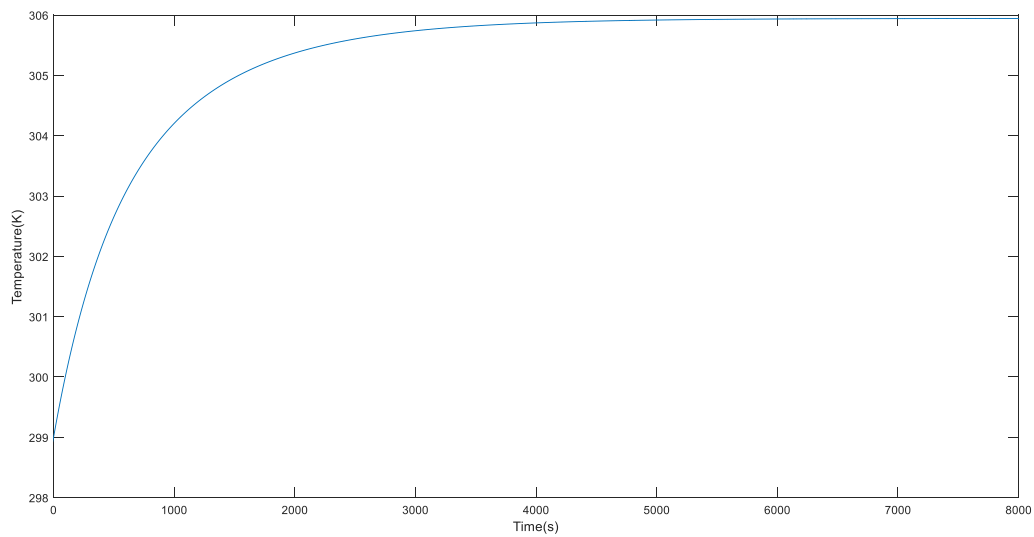


Figure 21. Temperature in the charge process

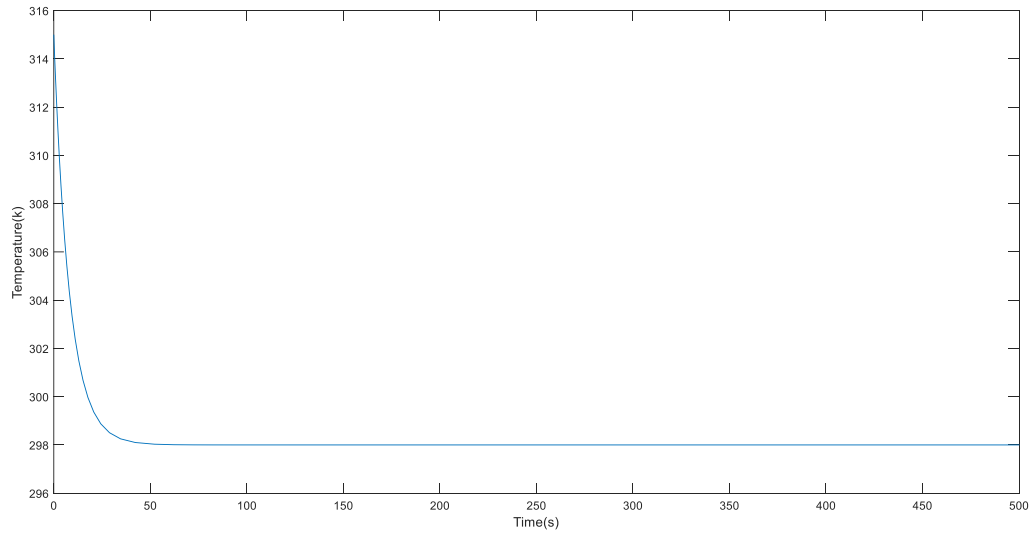


Figure 22. Temperature in the discharge process..

5.6. Fuel cell

The fuel cell is a device that converts chemical energy of a fuel into electricity through a reaction of positively charged hydrogen ions with oxygen or some other oxidizing agent. Fuel cells differ from batteries because they require a continuous source of fuel and oxygen to maintain the chemical reaction.

There are many types of fuel cells, but they are all composed of an anode, a cathode and an electrolyte that allows the positively charged hydrogen ions to move between the two parts of the fuel cell. The fuel cells are constituted by several individual cells connected electrically in series.

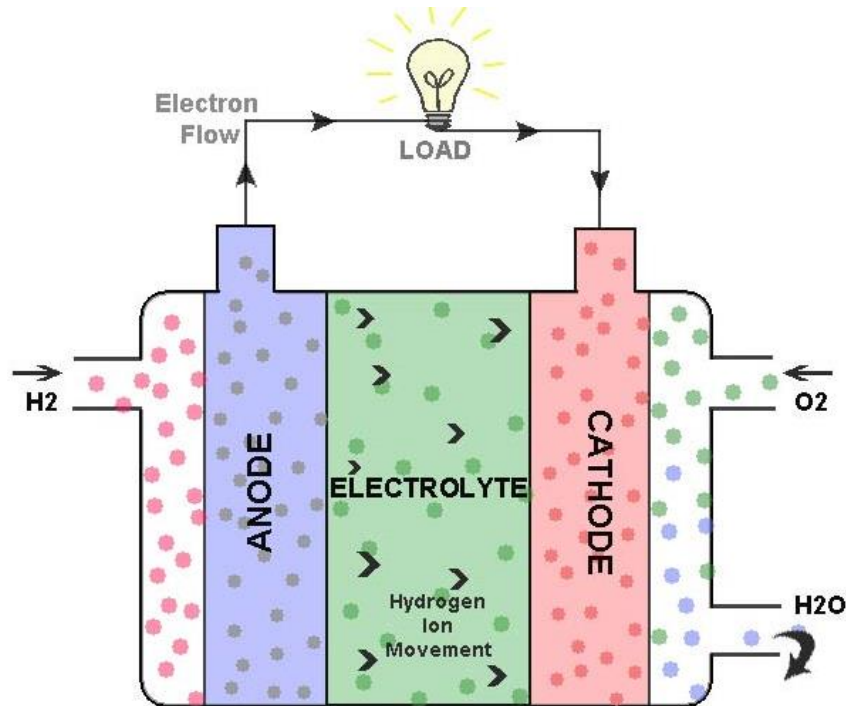


Figure 23. Fuel cell model

We are going to study proton exchange membrane fuel cell (PEM). These have been developed for transport applications as well as stationary applications. Its main features include low temperature ranges (50 to 100 °C) and a polymer electrolytic membrane. The PEM are the main candidates to replace the old alkaline fuel cells.

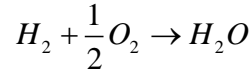
We will describe the elements that make it up:

- **Electrolyte:** It has several important functions, such as ionic conductor, electronic insulation and separator of the anodic and cathodic reactants. To maintain the balance of charges between the cathode and the anode the boundaries must pass through the membrane.
- **Gas diffusion layers:** Basically they are responsible for the distribution of the reactants to the surface of the electrode and to eliminate the products of the reaction.
- **Electrodes:** These must allow the contact between the reacting gas, the electrolyte or membrane and the electrode itself. These electrodes are divided in two, the first is a layer with the catalyst and the second is a layer formed by the porous medium.
- **Flow channels:** Flow channel plates ensure the distribution of both fuel and oxidant throughout the cell.

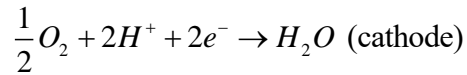
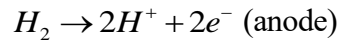
5.6.1. Fuel cell model

We will describe the mathematical model of the fuel cell. A PEM type cell transforms the chemical energy released during the electrochemical reaction of hydrogen and oxygen into electrical energy.

The general expression of the reaction is:



And the semi-reactions involved in the process are:



5.6.2. Electrochemical model

The voltage drop that is established in the stack is the product of several behaviors conditioned by the physical characteristics of the same, which can be differentiated by the following sums (Luis Valverde, 2013):

$$V_{fc} = v_o - v_{act} - v_{ohm} - v_{conc}$$

V_o is the open circuit voltage, which decreases according to the current requested by the circuit. V_{act} is the overvoltage activation, V_o decreases to this value in the first phase of the stack. Then, as the current increases, we are in the phase of ohmic losses (V_{ohm}). Finally, when the current is at maximum there is a sudden drop of voltage.

The polarization curve is described as:

$$V_{st} = n_{fc} V_{fc}$$

$$V_{fc} = x_1 + x_2(T_{st} - T_{st}^0) + x_3(0.5 \ln(P_{O_2,ca}) + \ln(P_{H_2})) - x_4(1 - \exp(-j / x_5)) - x_6 j - x_7 j^{(1+x_8)}$$

$$j = \frac{I_{st}}{A_{fc}}$$

Where

V_{st} is the final voltage in the fuel cell (V)

n_{fc} is the number of cell

V_{fc} is the voltage of the stack (V)

I_{st} is the current in the stack (A)

A_{fc} is the effective area of the membrane (cm^2)

j is the current density in the stack ($A\ cm^2$)

T_{0st} is the nominal stack temperature (K)

T_{st} is the stack temperature (K)

$P_{O_{2,ca}}$ is the oxygen pressure at the cathode (bar)

P_{H_2} is the hydrogen pressure at the anode (bar)

To calculate the expression of the voltage, we must calculate some coefficients x_i . To calculate these coefficients, we need experimental coefficients and 4 experimental points (p_{ji} , p_{ij}) that define the shape of the polarization curve. Calculating these points experimentally adds an unnecessary level of complexity to this work, so we get them from the manufacturer.

$$x_8 = \frac{1 + p_{4i}^2}{0.25 p_{4i}}$$

$$x_7 = \frac{(p_{4v} - p_{3v}) + (p_{2v} - p_{3v})(p_{4i} - p_{3i}) / (p_{3i} - p_{2i})}{-p_{4i}^{(1+x_8)} + p_{3i}^{(1+x_8)}(p_{4i} - p_{3i}) / (p_{3i} - p_{2i})}$$

$$x_6 = \frac{(p_{2v} - p_{3v}) - x_7 p_{3i}^{(1+x_8)}}{(p_{3i} - p_{2i})}$$

$$x_5 = \frac{p_{2i} - p_{1i}}{4}$$

$$x_4 = p_{1v} - p_{2v} - x_6 p_{2i}$$

$$x_3 = 2 p_{O_{2,ca}}^0 \frac{\Delta V_{fc}}{\Delta p_{O_{2,ca}}}$$

$$x_2 = \frac{\Delta V_{fc}}{\Delta T_{st}}$$

$$x_1 = p_{1v} - x_3 (0.5 \ln(P_{O_{2,ca}}^0) + \ln(p_{H_{2,ca}}))$$

Table 6. X_i coefficient

X_i	Valor
X1	1.0461
X2	0.00293
X3	0.24352
X4	0.066098
X5	0.012705
X6	0.29179
X7	0.028396
X8	8.0011

The hydrogen required to produce power is given by the following expression:

$$\dot{n} = \frac{n_{cell} - I}{zF}$$

Where

\dot{n} is the hydrogen flow rate demanded ($mol \cdot s^{-1}$)

N is the number of cells in the fuel cell

I is the electric current (A)

Z is the number of electrons per molecule (2)

F is the Faraday constant (96500)

5.6.3. Simulink implementation

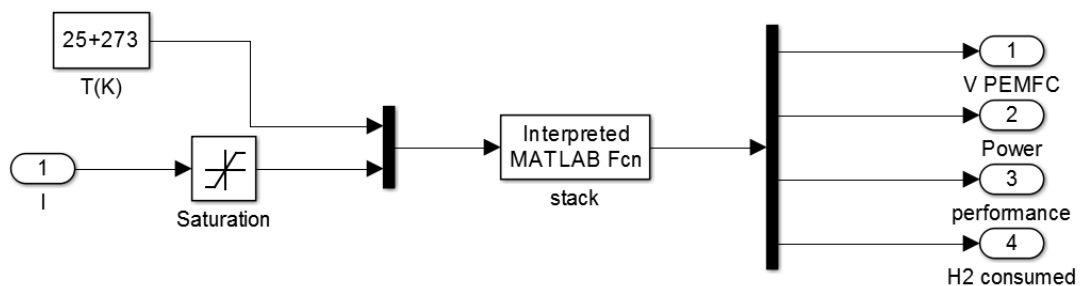


Figure 24. Simulink fuel cell model

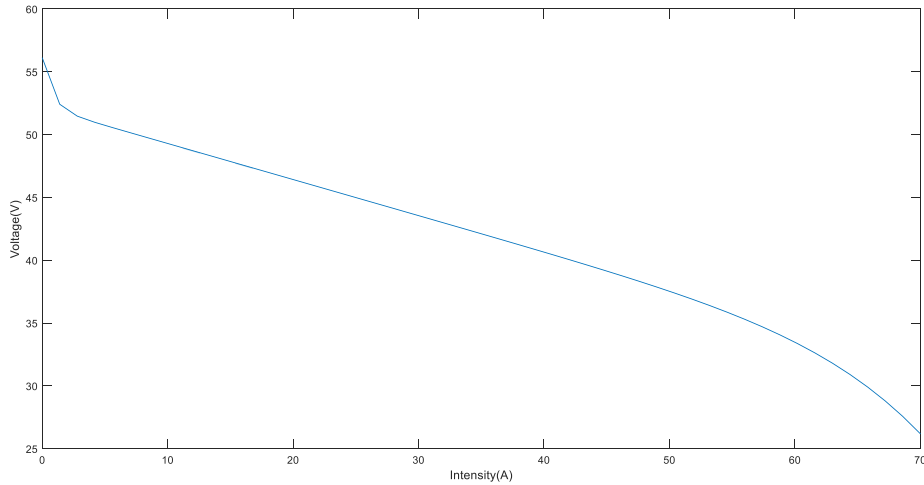


Figure 25. Fuel cell I-V curve

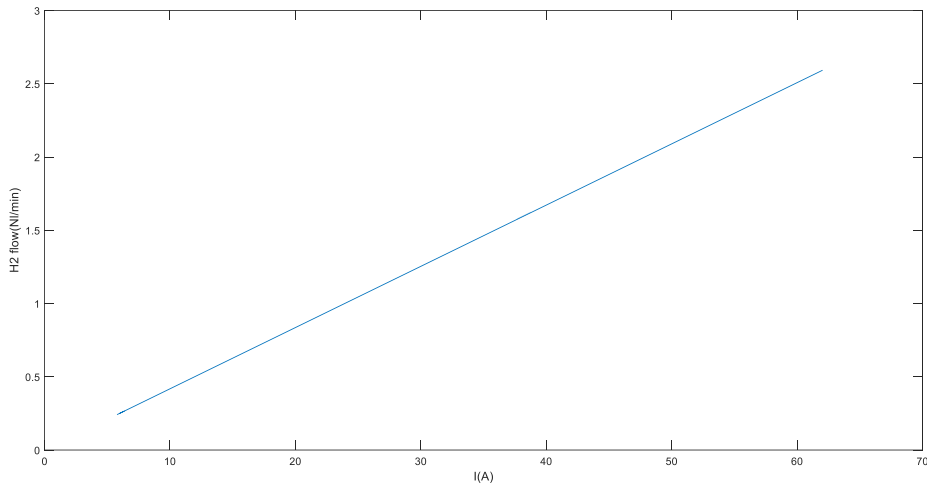


Figure 26. Hydrogen flow consumed.

5.7. Stationary Battery

The battery is a device that stores energy converting chemical energy directly to electrical energy.

A battery is made up of a few voltaic cells. Each cell consists of two half cells connected in series by a conducting electrolyte containing anions and cations. One part contains the negative electrode (the electrode to which the anions migrate) while the other part contains the positive electrode (the electrode to which the cations migrate).

Redox reactions charge the battery. During the charge of the battery the cations are reduced because the electrons are added, while the anions are oxidized because the electrons are removed. During the discharge, this process is reversed.

Each half cell has an electromotive force (Emf) determined by its ability to conduct electrical current from the inside to the outside of the cell. The Emf of the complete cell is the difference between the Emfs of its half cells.

The voltage between the terminals of the cell is known as the voltage difference and is measured in volts. This voltage difference in a cell that is not being charged or discharged is called the open circuit voltage and is equal to the emf of the cell. Due to the internal resistance, the voltage of a cell being discharged is less in magnitude than the open circuit voltage and conversely, the voltage of a cell being charged exceeds the open circuit voltage.

We are going to work with the lead-acid battery. This is a very common type of battery in vehicles, used as a starter battery, although they it is also used as electric vehicle's traction battery. It usually provides a voltage between 6-12V.

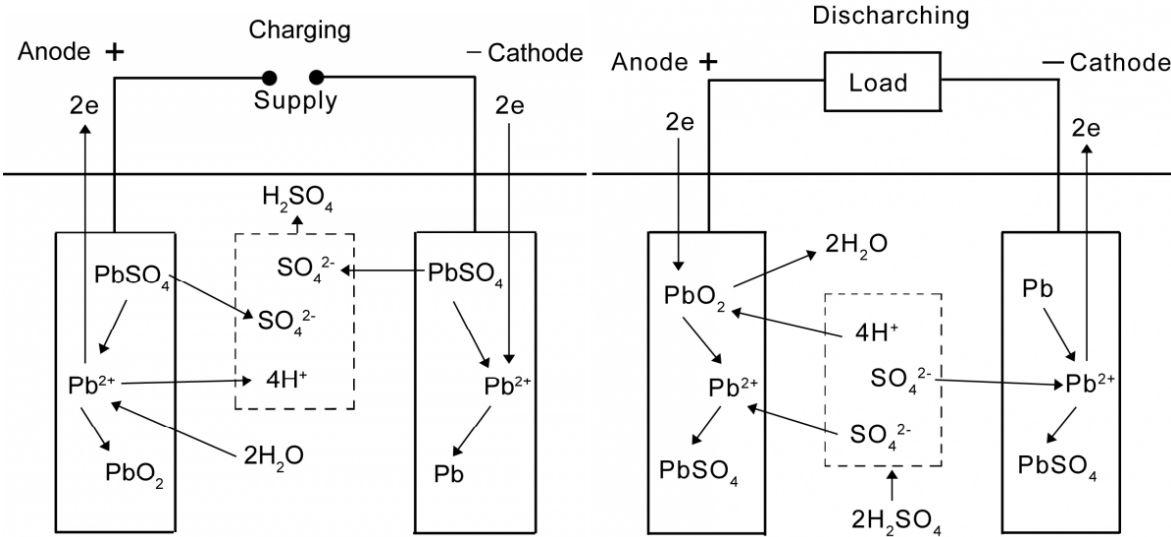


Figure 27. Scheme for loading and unloading a lead-acid battery

The lead-acid battery is one of the most used accumulator in the present thanks to its low cost. In the battery, the two electrodes are made of lead and the electrolyte is a solution of distilled water and sulfuric acid. When the battery is charged, the positive electrode has a deposit of lead dioxide and the negative electrode is lead. As the chemical process releases gases (hydrogen and oxygen) the system needs to be ventilated to the outside

5.7.1. Stationary Battery model

For this work, we use a dynamic model for lead-acid batteries. In the following figure we see the equivalent circuit for the battery:

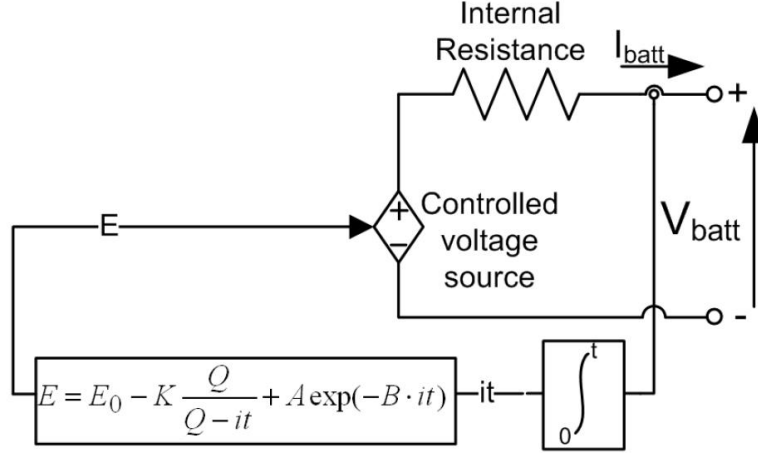


Figure 28. Electrical schematic for the battery model

The voltage of the battery for the charging process is described by the following equation:

$$V_{bat} = V_{bt,0} - K_{bt} \frac{C_{120,bt}}{C_{120,bt} - C_{out,t}} I_{bt} - K_{bt} \frac{C_{120,bt}}{C_{120,bt} - C_{out,t}} C_{out,t} + A_{bt} e^{-B_{bt} C_{out,t}} - R \cdot I_{bt}$$

$$C_{out,t} = \int_0^t I_{bt} dt$$

And for the discharge process, the battery voltage is described by:

$$V_{bat} = V_{bt,0} - K_{bt} \frac{C_{120,bt}}{C_{out,t} + 0.1 C_{120,bt}} I_{bt} - K_{bt} \frac{C_{120,bt}}{C_{120,bt} - C_{out,t}} C_{out,t} + A_{bt} e^{-B_{bt} C_{out,t}} - R \cdot I_{bt}$$

Where

$V_{bt,0}$ is the open circuit battery voltage.

$C_{out,t}$ is the current capacity of the battery (Ah)

A_{bt} is the amplitude of the exponential zone (V)

B_{bt} is the inverse of the time constant in the exponential zone (Ah^{-1})

K_{bt} is the polarization constant (V)

$C_{120,bt}$ is the maximum capacity of the battery (Ah)

With the equations and the coefficients of the following table that are obtained experimentally we can simulate the behavior of the battery.

Table 7. Parameters of the lead-acid battery model

Parameter	Value
C120,bt	367Ah
Vbt,0	51.58 V
Kbt	0.006215 V
Abt	11.053 V
Bbt	2.452 Ah ⁻¹
R	0.07 Ω

5.7.2. Simulink implementation

We are going to obtain the evolution of battery voltage while it is being discharged. To do this, we are going to subject the battery to a constant current demand. This signal will be a current step at 25 Amps to obtain stationary conditions.

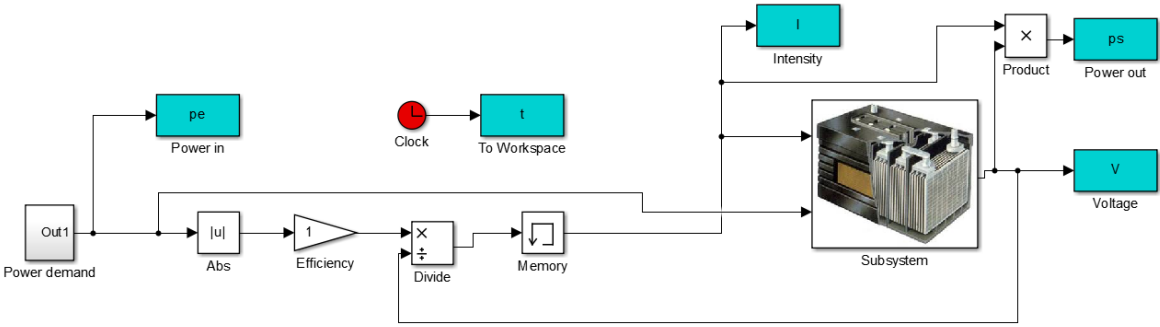


Figure 29. Simulink battery model

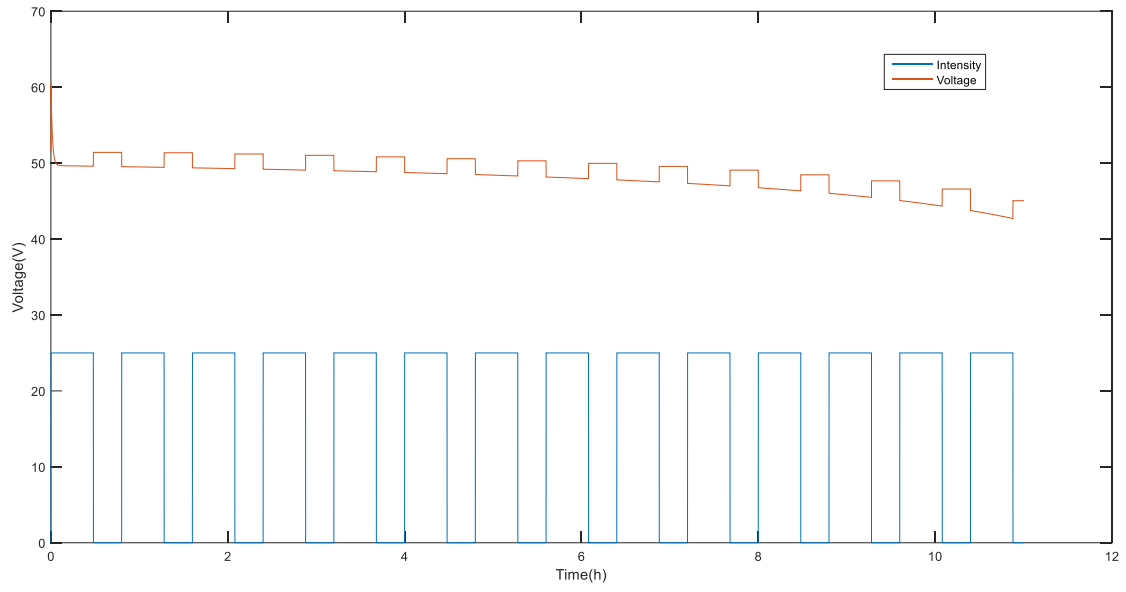


Figure 30. Output voltage of the battery against current step

CHAPTER 3

Complete system and user interface

Index

3.1 Energy demand model	51
3.2 Control system model	52
3.3 Complete model	55
3.4 User interface	55

In this section we are going to build the whole system. To do this, we must do a previous study of energy demand in Spain and then create a controller. Finally, we will create a graphical interface where the user can activate the power generation and storage systems to analyze the microgrid simulations.

6.1. Energy demand model

For the simulations of the complete system we need a reference of power demand. To do this, we will take real data from Red Eléctrica de España.

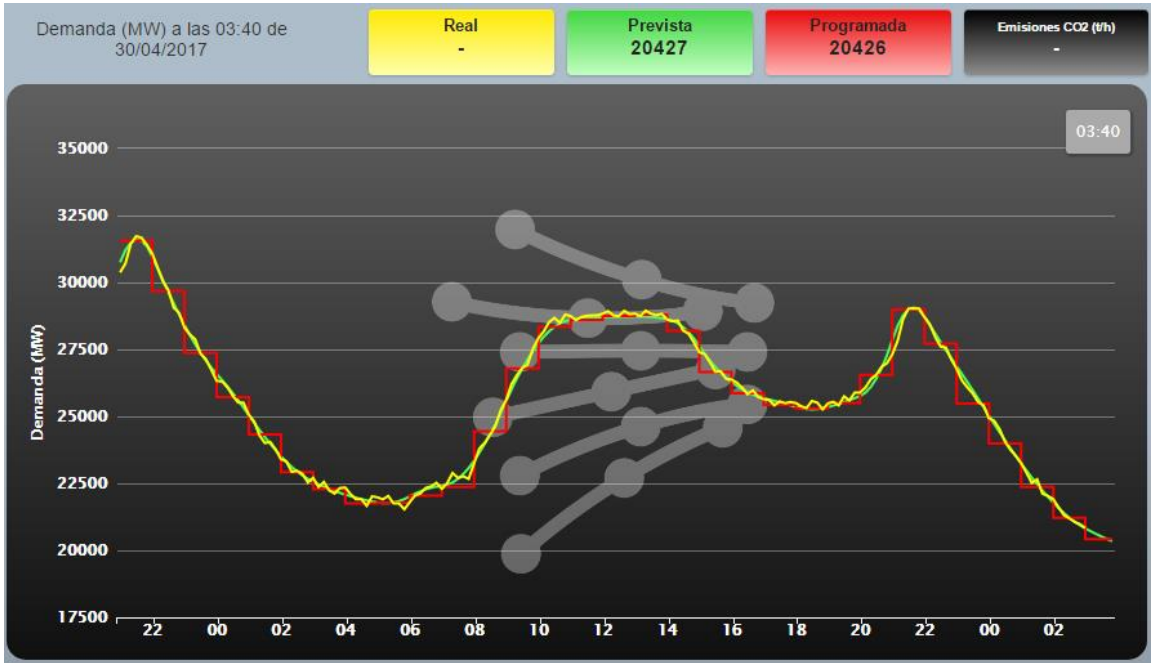


Figure 31. Electric energy demand in Spain. Source: Red eléctrica Española.

The previous graph shows the energy consumption in real time. Between the expected consumption and the real consumption there are not many variations. For our system, we will use the average demand for electric power in a family home.

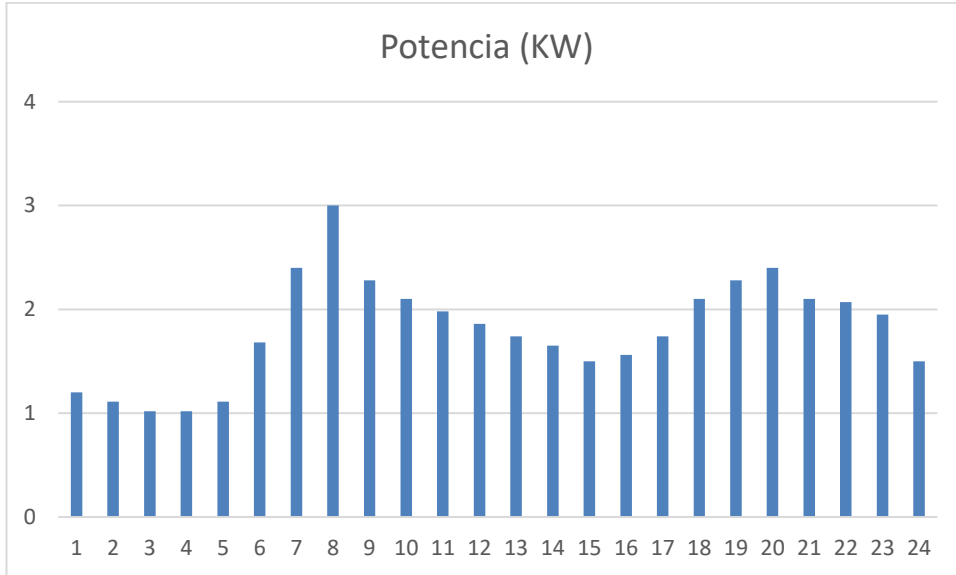


Figura 32. Power demand for an average home

6.2. Control system model

The control system will manage the entire network. The control system is responsible for connecting the signals to each block for proper operation.

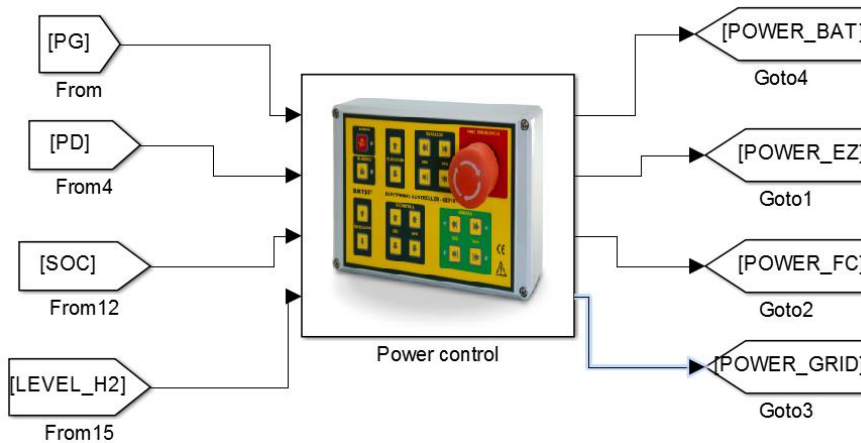


Figure 33. Control system.

The control scheme is as follows:

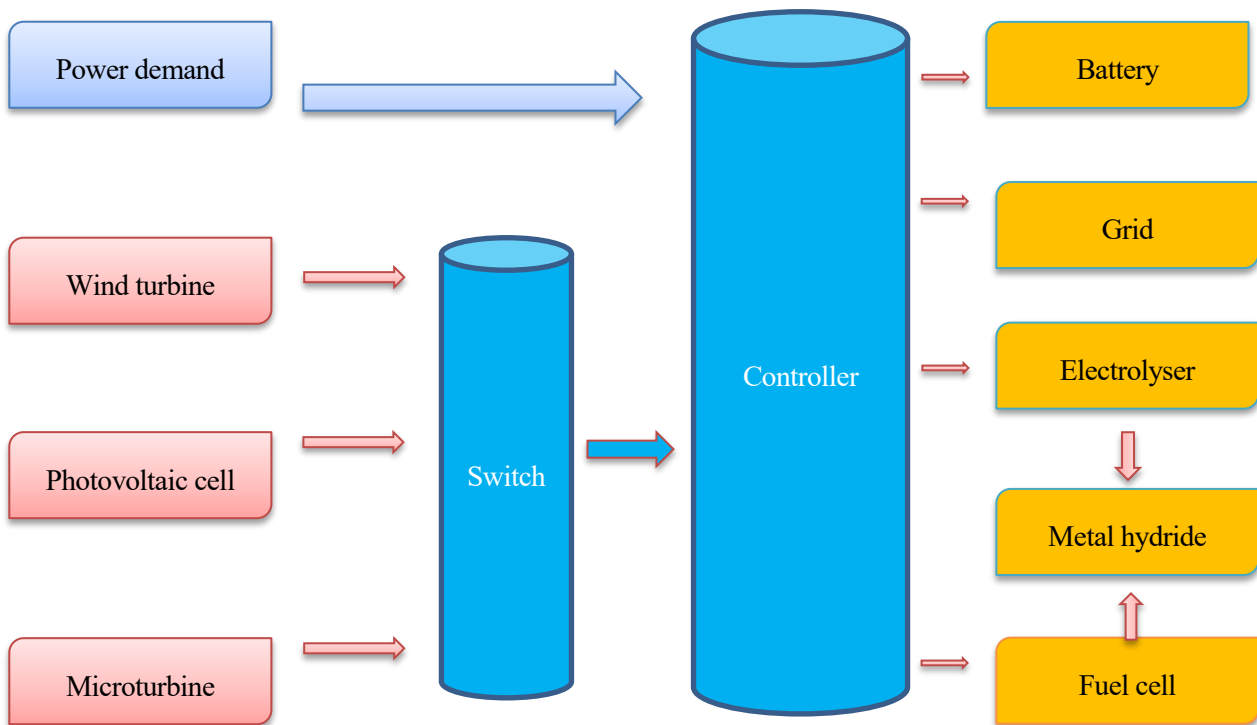


Figure 34. Schematic of network operation.

The controller is divided into two parts. The first, called "Switch", is responsible for deciding which generation systems deliver their power to the complete system. This is decided beforehand by the user through a graphical interface, which we will see later

The second, called "Controller", will manage all the power of the system. Depending on the power demanded, the power generated and the systems that the user activated, the controller will take different control strategies. The strategies are:

- If the hydride is deactivated, the controller does not deliver power to either the fuel cell or the electrolyser. The controller disables them.
- If we charge 90% the battery and the electrolyser is activated, the electrolyser will start to store hydrogen in the hydride. If the battery is at 30% and we have the fuel cell, it will generate the necessary power.
- If there is electrolyzer without the battery, it will operate when the power generated is greater than the demanded.
- The hydride and the battery begin at 50% of its load, so if we only activate the fuel cell and the hydride, it will run until the hydride is exhausted.

- If the system generates a lot of power and we can not store it, the energy will be sold to an electrical grid. We can also buy energy in case the demand is very high and our system does not have accumulated energy.

We are going to representate the most difficult case:

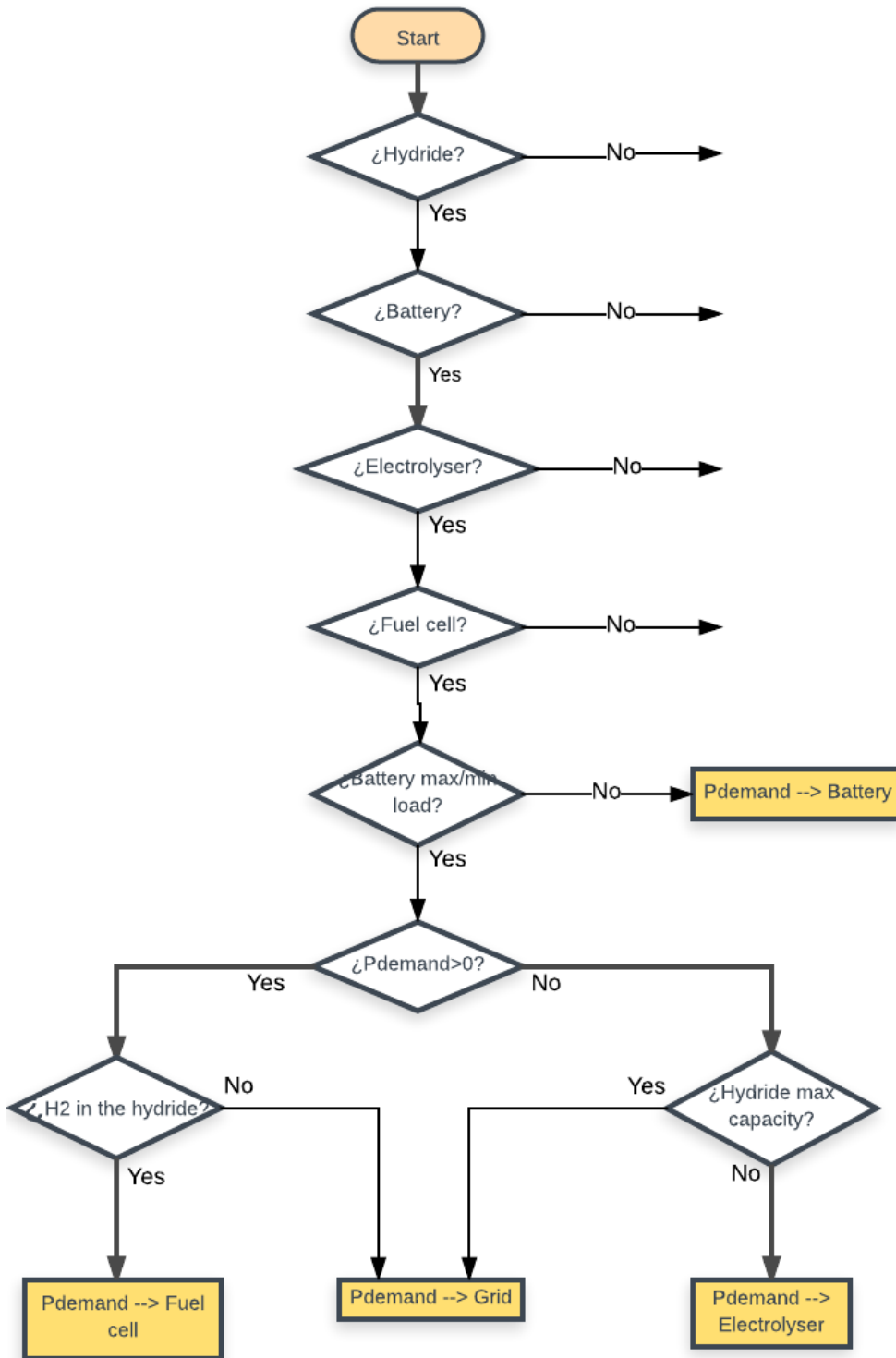


Figure 35. Flowchart

6.3. Complete model

The main goal of our work was to integrate all the sub-models and analyze the results. In this section, we will indicate how this objective has been achieved.

The integration of all blocks is a complicated task. We must join all the variables correctly, make an appropriate use of the simulation time and be careful with the integration variables.

It is very important to give initial values to the integrators and the memory blocks. We use the memory blocks because the input to a model is its same output (as in the electrolyzer, which calculates the current with the power and its own output voltage).

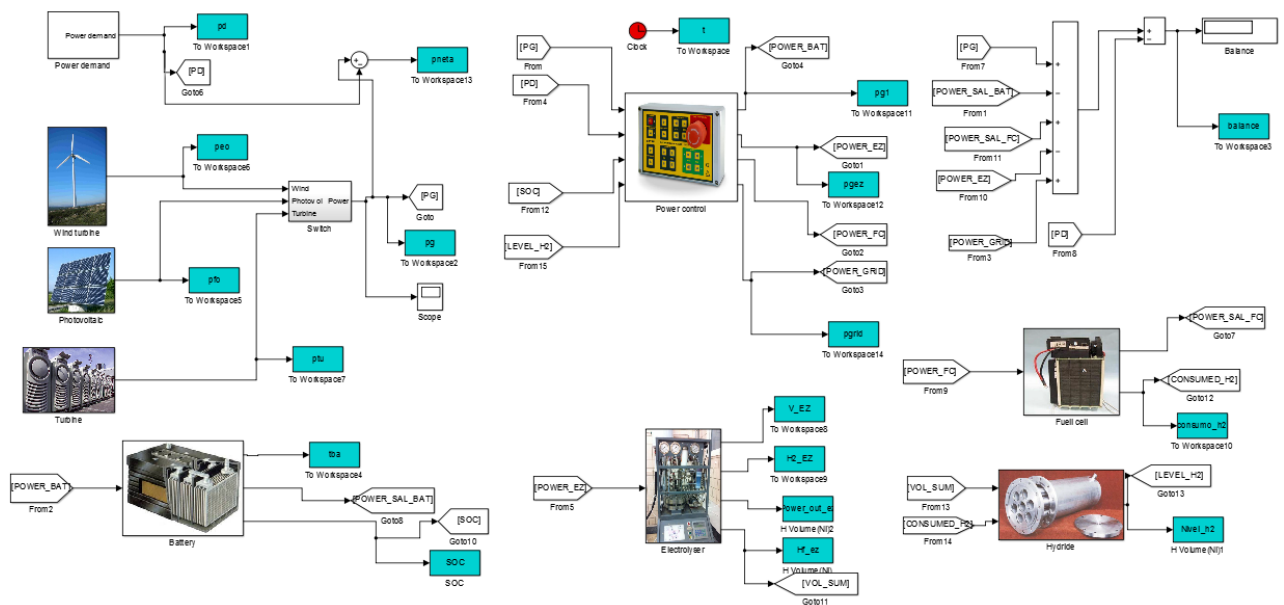


Figure 36. Complete system.

We have a wind turbine, photovoltaic cells and a microturbine that are power generation systems. The inputs of the controller are the generated power, the demanded, and the load levels in the hydride and the battery. The controller sends power signals to the fuel cell, battery, and electrolyser. For the hydride, its inputs are the demand for hydrogen by the fuel cell and the amount of hydrogen generated by the electrolyser.

6.4. User Interface

The user decides how many sub-models are active in each simulation. To do this, we have created a GUI interface with the Matlab GUIDE tool.

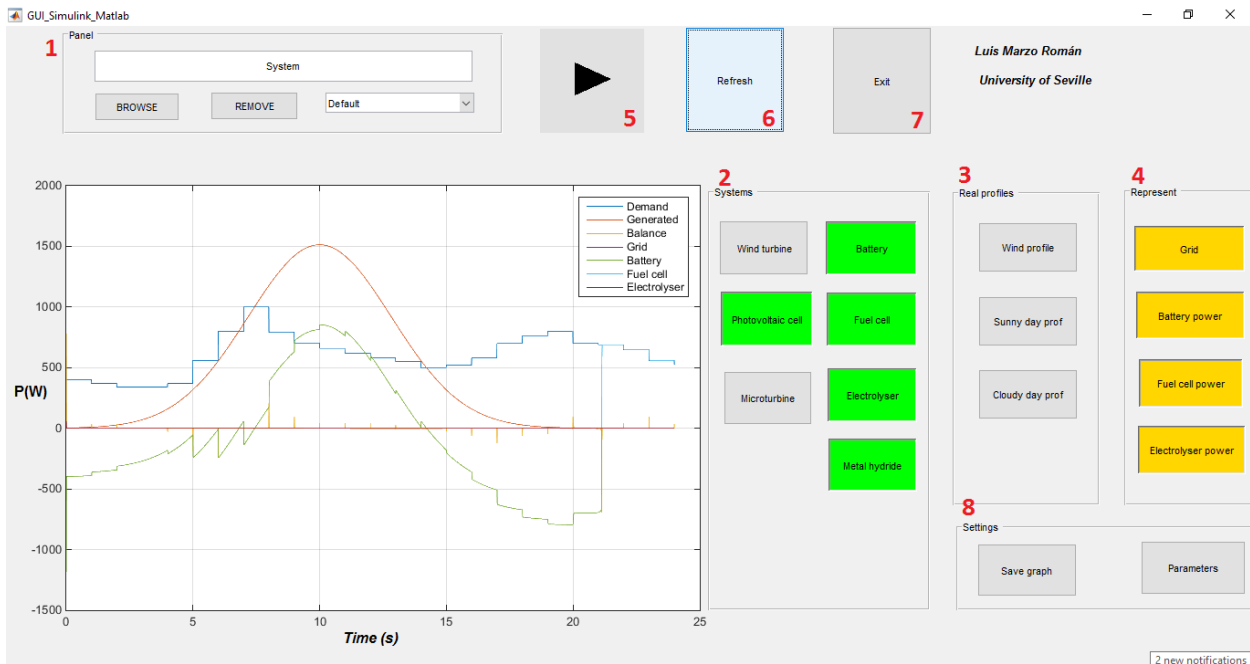


Figure 37. User interface

1. **Panel:** In this panel we have a first button to search in the directory our simulink model, a second button to remove it and the third is a pop-up menu with several initial configurations for the system.
2. **Systems:** These buttons are the blocks that we can activate or deactivate in our system. Depending on which ones are active, the controller will take some actions or others.
3. **Real profiles:** These are three real power generation profiles in 24 hours.
4. **Represent:** Buttons to select the systems that we want to see in the graph.
5. **Play button.**
6. **Refresh:** We click this button every time we want to see the graph updated.
7. **Exit button.**
8. **Settings:** The first buttons allow you to save and modify the graph. The second, when it is pressed, we enter in a second GUI where we can choose the parameters of each model individually. In addition we can permanently save our new parameters in a .mat file.

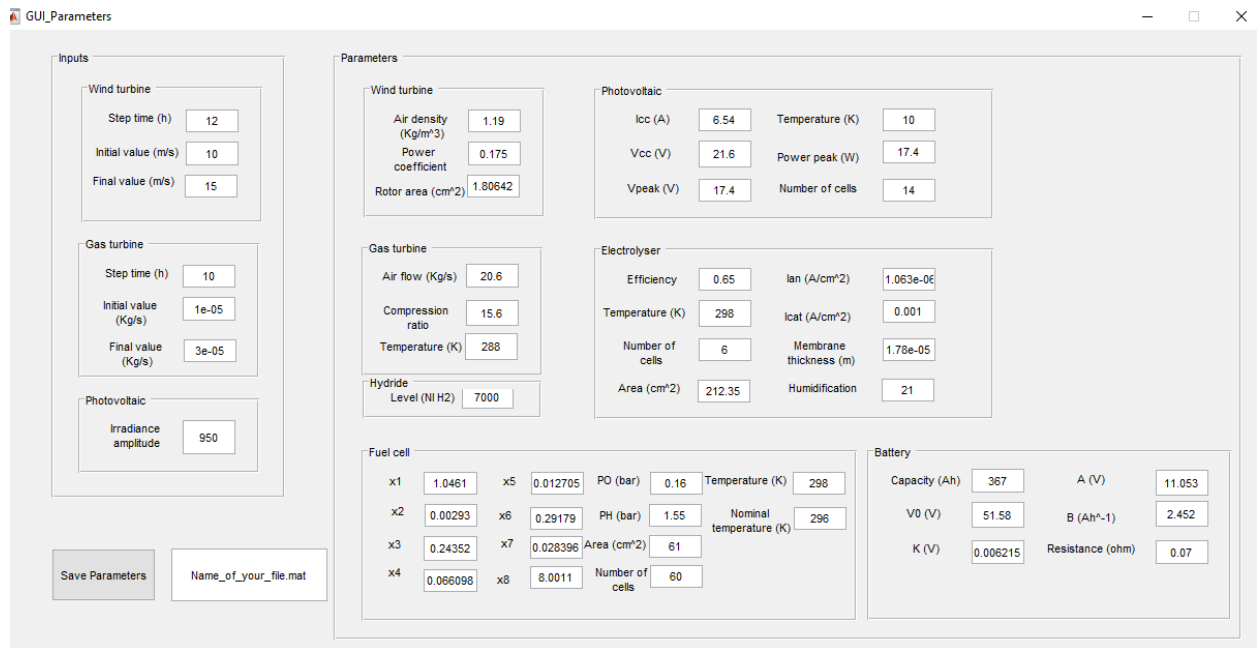


Figure 38. User interface parameters.

CHAPTER 4

Analysis and conclusions

Index

4.1 Analysis	59
4.2 Conclusions	64

In this section we will check the controller. To do this, we will subject the system to several types of simulation.

7.1. Analysis

In the system, 7 individual blocks can be activated or deactivated, so we have 128 different types of possible simulations. However, the metal hydride plays a key role, and if it is not present in the simulation the fuel cell and the electrolyzer do not operate. For the simulations, the battery and the hydride are initialized to half of their maximum load.

❖ *Photovoltaic cell, battery, electrolyser and metal hydride.*

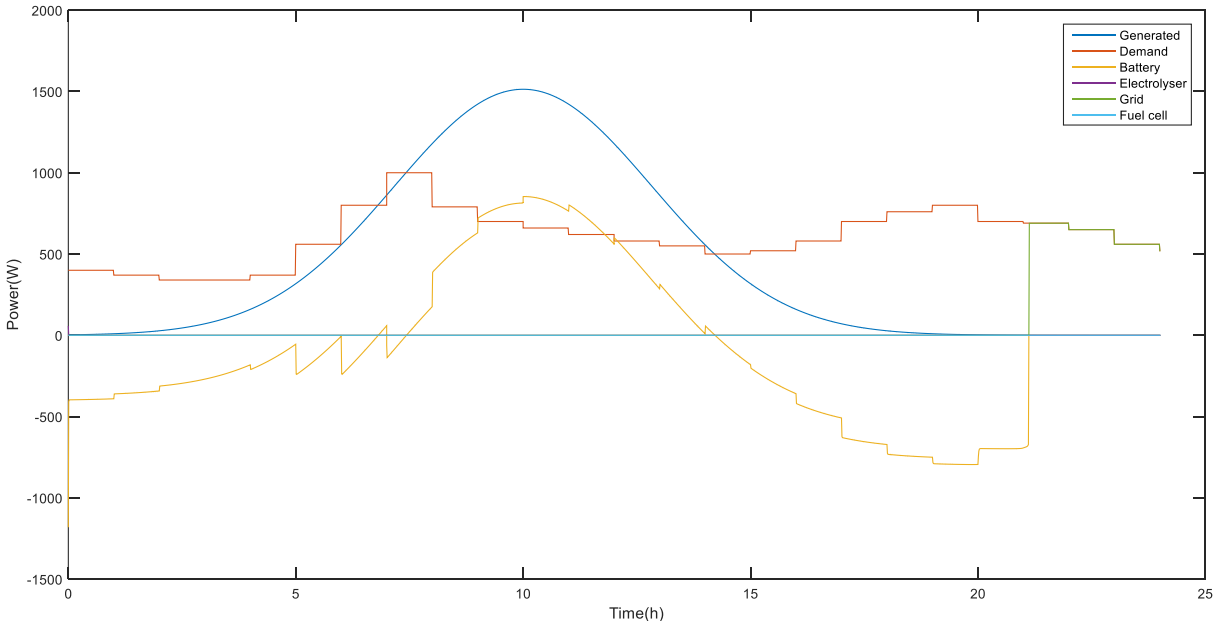


Figure 39. First system simulation

If the power generated is greater than the demanded, we store this energy in the battery. If there is no fuel cell, when the battery is discharged at 22h, no other system can supply power to the system, and therefore we buy energy to an electrical grid.

❖ *Photovoltaic cell, battery, electrolyser, fuel cell and metal hydride.*

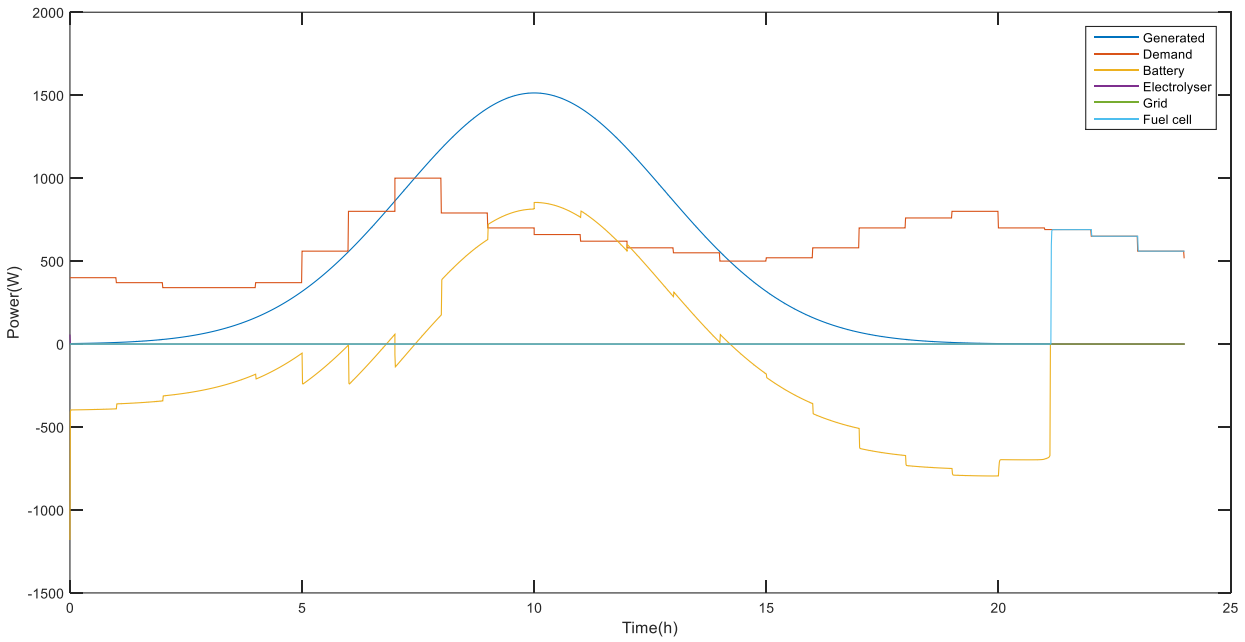


Figure 40. Second system simulation

Here the fuel cell is activated, and the system does not go into negative balance thanks to the fuel cell provides the remaining energy.

❖ *Photovoltaic cell, microturbine, battery and fuel cell.*

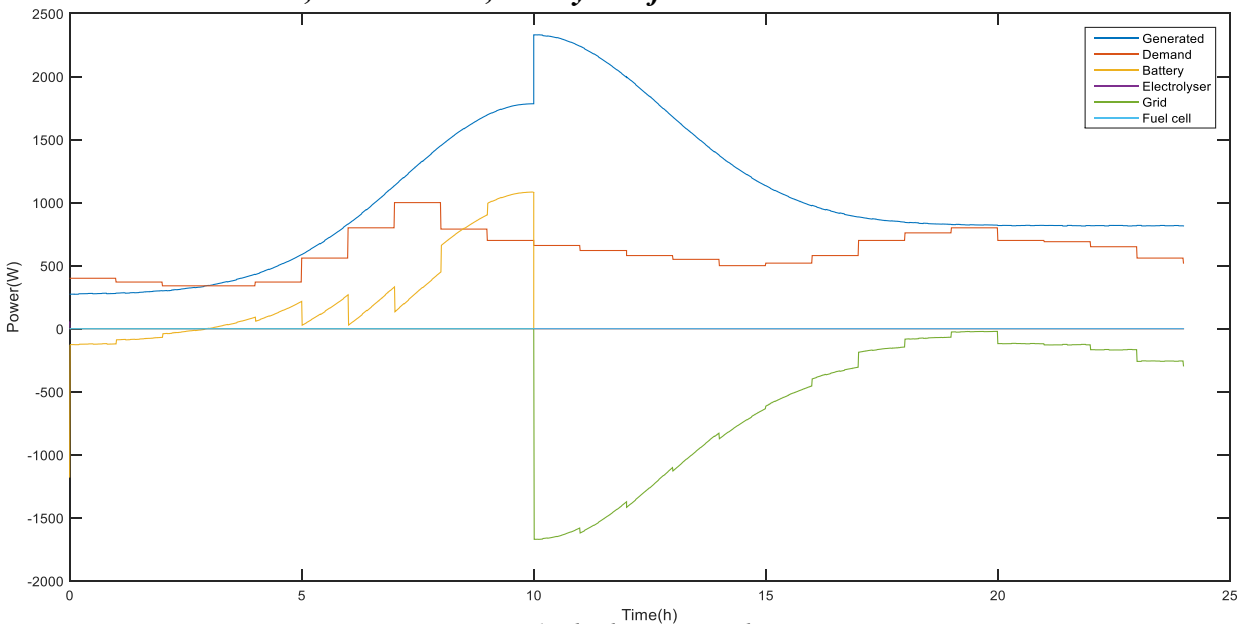


Figure 41. Third system simulation

In this simulation we have the microturbine, and with it we manage to charge the whole battery. However, since we do not have an electrolyser, we have to sell the energy into an electrical grid. We can see a step in the power generated. This is because at 10 hours we increase fuel flow in the turbine.

❖ **Photovoltaic cell, microturbine, battery, electrolyser, fuel cell and metal hydride.**

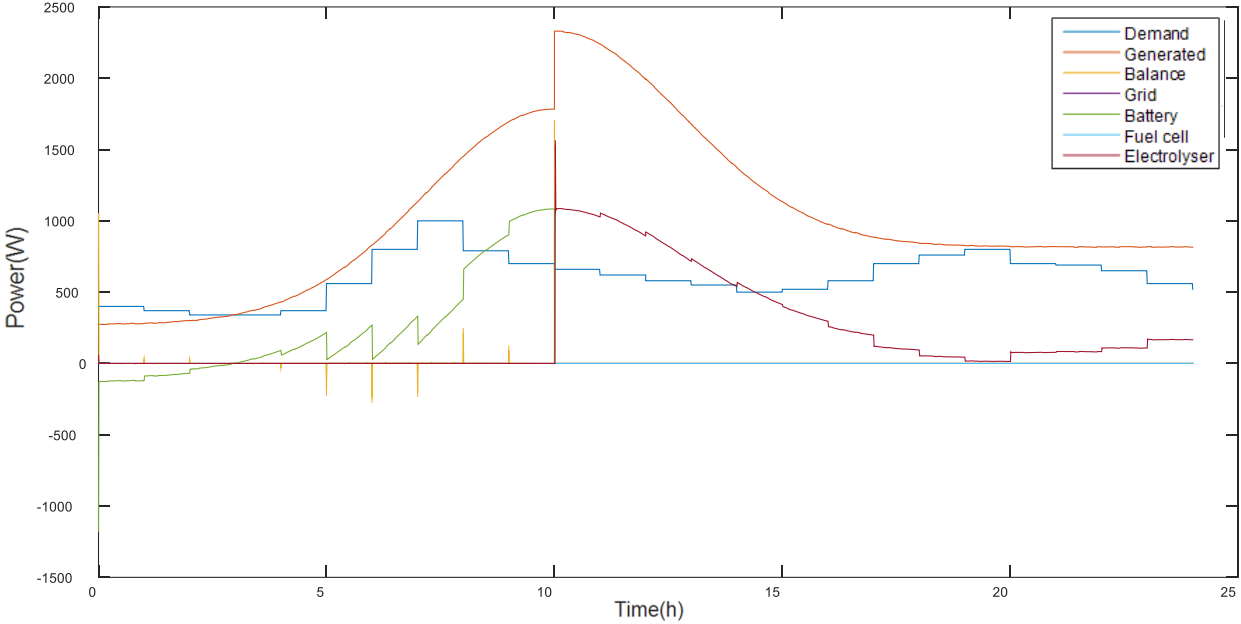


Figure 42. Fourth system simulation

This is the same simulation as the previous one but solving the problem of positive balance. The electrolyser consumes power and generates hydrogen which is stored in the hydride.

❖ **Microturbine, battery, electrolyser, fuel cell and metal hydride.**

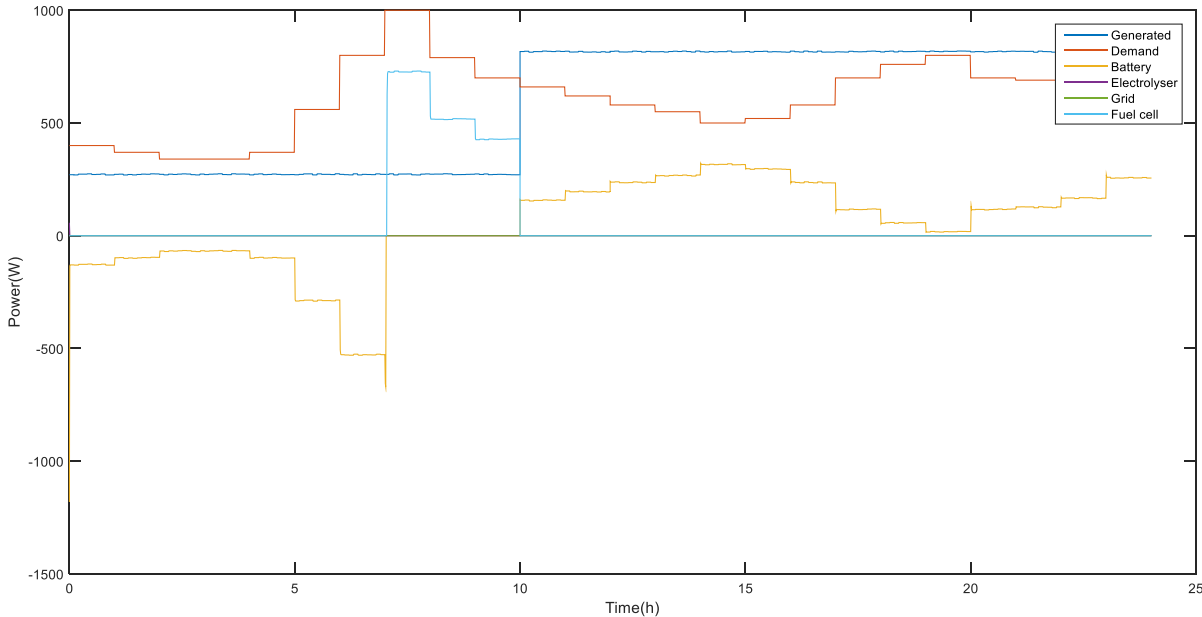


Figure 43. Fifth system simulation

When the battery is discharged, the system uses the fuel cell. When the microturbine starts to generate more power than the demanded, we begin to store energy in the battery.

❖ *Microturbine, wind turbine, battery, electrolyser, fuel cell and metal hydride.*

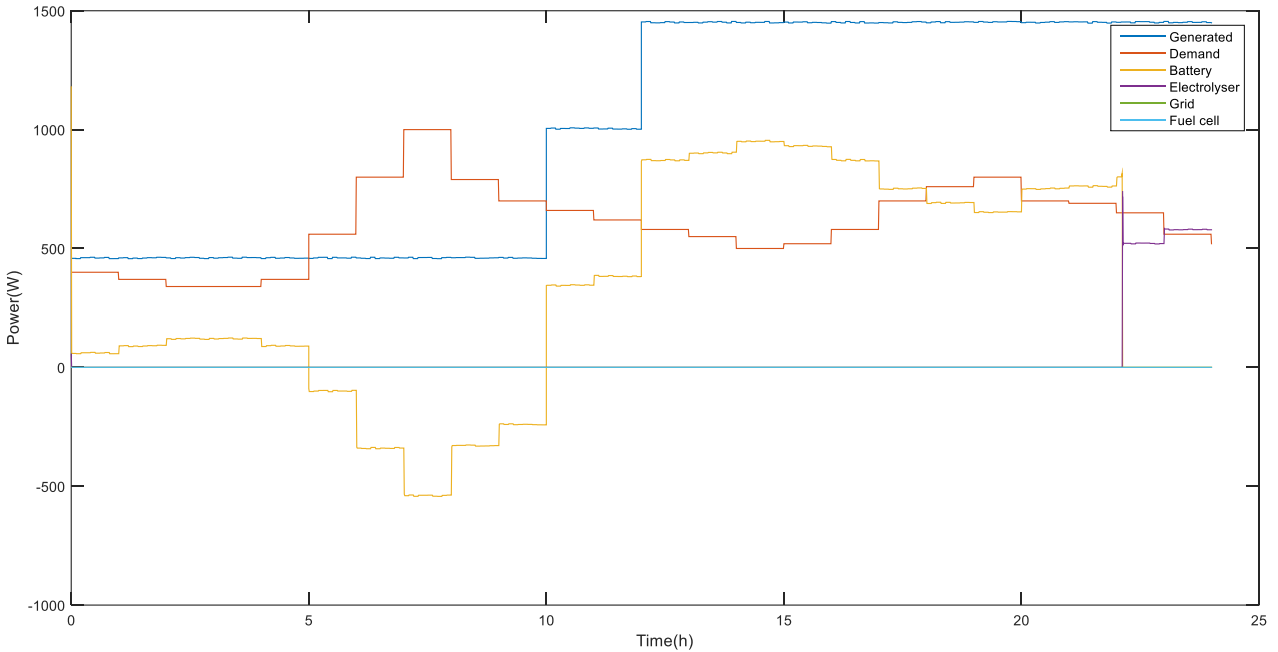


Figure 44. Sixth system simulation

The wind speed change at 10 hours and the amount of fuel in the turbine change at 12 hours. The electrolyser produces hydrogen when the battery is charged.

❖ *Photovoltaic cell, electrolyser, fuel cell and metal hydride.*

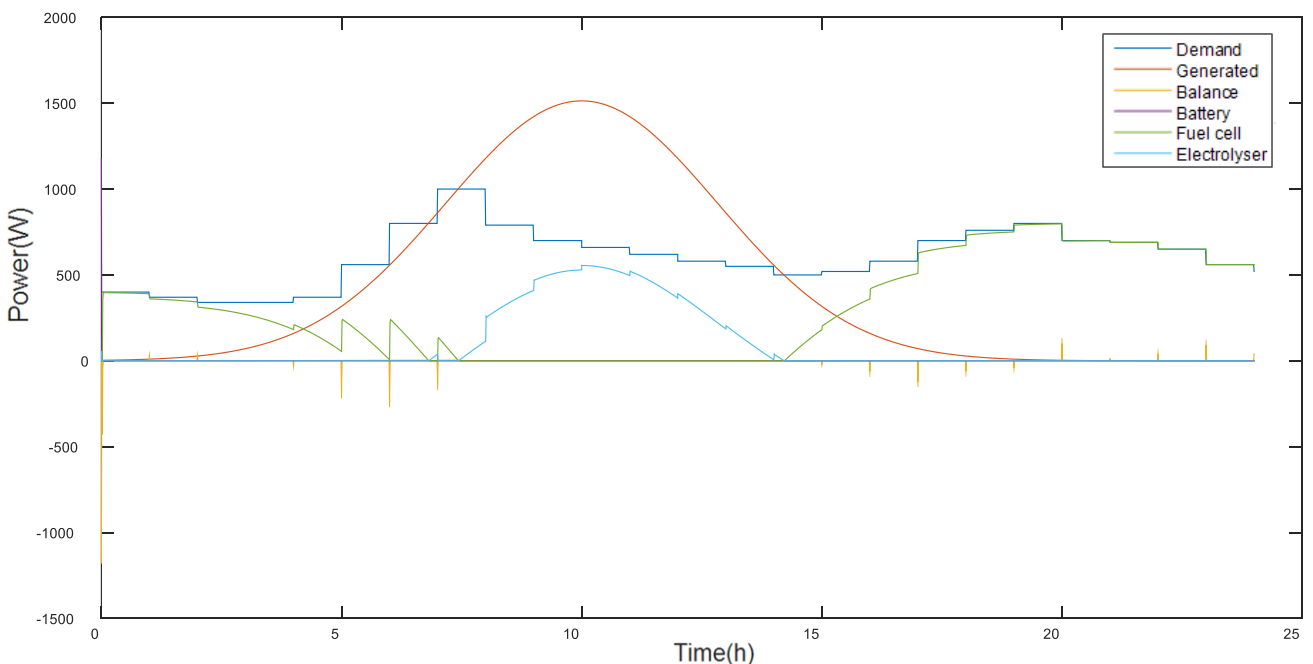


Figure 45. Seventh system simulation.

Here we do not have battery. It is observed that during a day the system is stable with the fuel cell, the hydride and the electrolyser. If we simulate a whole week, the hydride would exhaust and we would use the electrical grid.

❖ *Real wind profile, battery, electrolyser, fuel cell and metal hydride.*

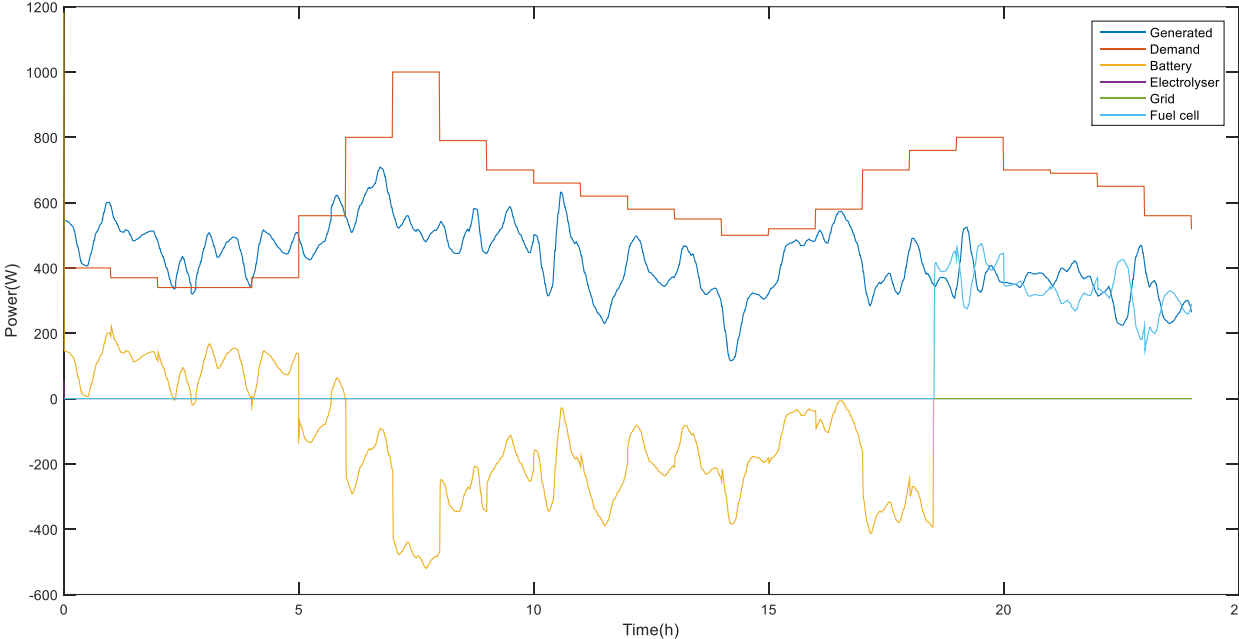


Figure 46. Real wind profile.

This is a real wind profile. When the battery is discharged, the fuel cell generates the necessary power.

❖ *Real cloudy day profile, battery, electrolyser, fuel cell and metal hydride.*

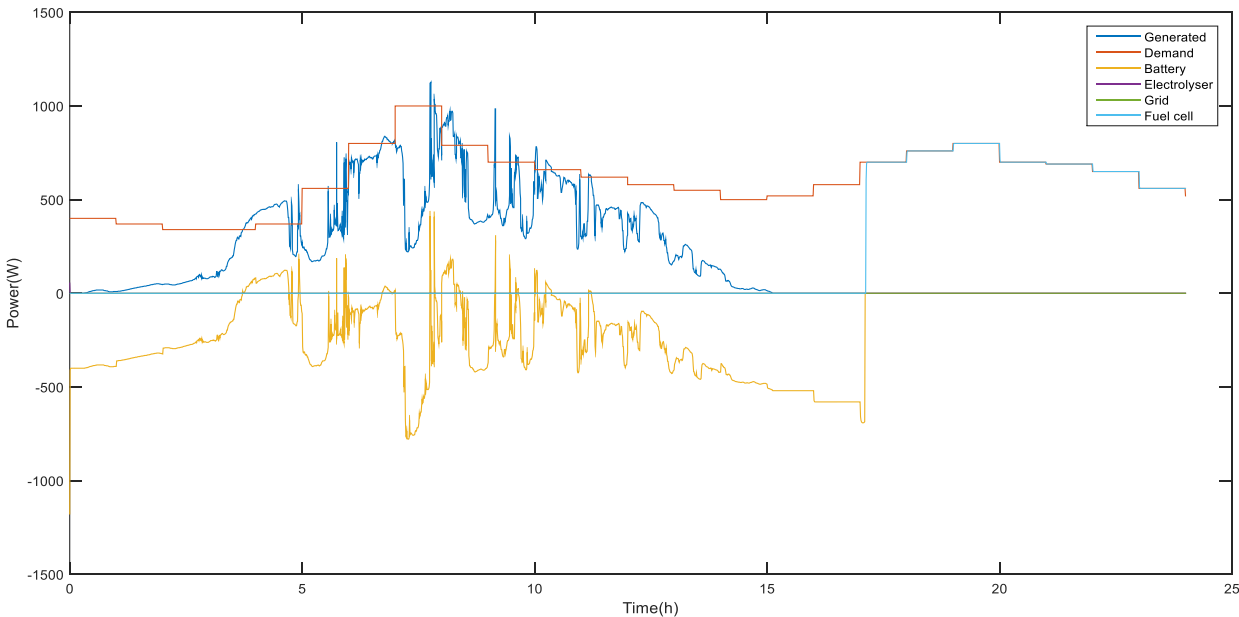


Figure 47. Real cloudy profile.

This is a real cloudy day profile. In spite of the power peaks in the generated curve (blue), the microgrid works perfectly.

❖ *Real sunny day profile, battery, electrolyser, fuel cell and metal hydride.*

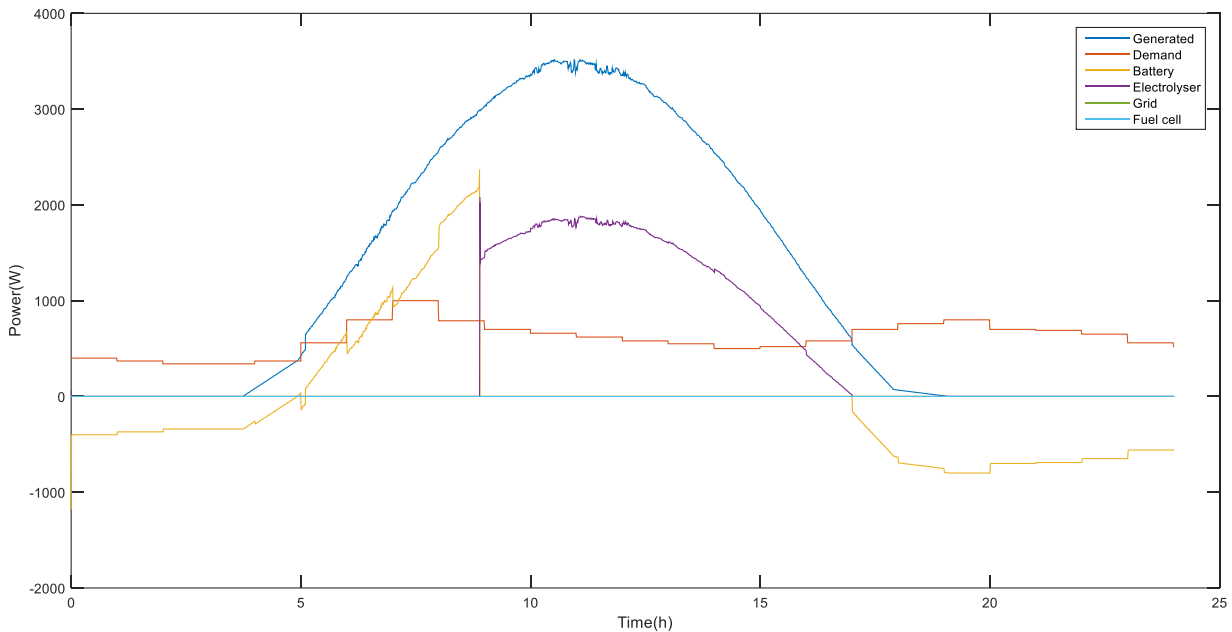


Figure 48. Real sunny profile.

This is a real sunny day profile. When the battery is discharged, the fuel cell generates the necessary power.

7.2. Conclusions

In this last chapter we have simulated a microgrid with renewable energy and storage based on hydrogen to see the operation of the controller. The previous simulations show a correct operation of the controller. The user interface works perfectly, it is easy to use and very flexible.

Finally, we must emphasize that the control system is correctly designed so that it can satisfy the demand of electrical energy with the physical restrictions of each sub-system.

BIBLIOGRAPHY

- [1] **Luis Valverde Isorna**, Gestión de energía en sistemas con fuentes renovables y almacenamiento de energía basado en hidrógeno mediante control predictivo [Tesis].
- [2] **A. Freni, F. Cipiti, G. Cacciola** Finite element-based simulation of a metal hydride-based hydrogen storage tank [Journal]
- [3] **Alejandro J. Del Real, Alicia Arce, Carlos Bordons** Hybrid model predictive control of a two-generator power plant integrating photovoltaic panels and Fuel Cell [Conference]
- [4] **F. J. Pino, Luis Valverde, Felipe Rosa** Influence of wind turbine power curve and electrolyzer operating temperature on hydrogen production in wind–hydrogen systems [Journal]
- [5] **Iranzo Alfredo** Desarrollo y validación experimental de un modelo computacional de pilas de combustible de tipo PEM y su aplicación al análisis de monoceldas [Book].
- [6] **M. Hashem, Nehrir Caisheng Wang** Modeling and control of fuel cells [Book].
- [7] **Melnichuk Maximiliano** Estudio numérico y experimental de almacenadores de hidrógeno basados en hidruros metálicos [Book].
- [8] **A. Awasthi, K. Scott, S. Basu**, Dynamic modeling and simulation of a proton exchange membrane electrolyzer for hydrogen production [Journal].
- [9] **O. Tremblay, L. Dessaint** A Generic Battery Model for the Dynamic Simulation of Hybrid Electric Vehicles [Journal]
- [10] **O.C. Onar, M. Uzunoglu, M.S. Alam** Modeling, control and simulation of an autonomous wind turbine/photovoltaic/fuel cell/ultra-capacitor hybrid power system [Journal]
- [11] **R. García-Valverde, N. Espinosa, A. Urbina** Simple PEM water electrolyser model and experimental validation [Journal]
- [12] **Rosa F.** Estudio teórico y experimental de la producción de hidrógeno a partir de un electrolizador alcalino [Journal].
- [13] **Ulleberg Oystein** Modeling of advanced alkaline electrolyzers: a system simulation approach [Journal]
- [14] **Toledo Velazques, Miguel. Lugo Reyes, Raúl.** Termodinámica de las turbina de gas [Book]